European Journal of Medicinal Chemistry 225 (2021) 113783

Contents lists available at ScienceDirect

European Journal of Medicinal Chemistry

journal homepage: http://www.elsevier.com/locate/ejmech

Discovery of 1-(phenylsulfonyl)-1*H*-indole-based multifunctional ligands targeting cholinesterases and 5-HT_6 receptor with anti-aggregation properties against amyloid-beta and tau

Tomasz Wichur [a], Anna Pasieka [a], Justyna Godyń [a], Dawid Panek [a], Izabella Góral [a], Gniewomir Latacz [a], Ewelina Honkisz-Orzechowska [a], Adam Bucki [a], Agata Siwek [a], Monika Głuch-Lutwin [a], Damijan Knez [b], Xavier Brazzolotto [c], Stanislav Gobec [b], Marcin Kołaczkowski [a], Raimon Sabate [d, e], Barbara Malawska [a], Anna Więckowska [a, *]

[a] *Faculty of Pharmacy, Jagiellonian University Medical College, Medyczna 9, 30-688 Kraków, Poland*
[b] *University of Ljubljana, Faculty of Pharmacy, Aškerčeva 7, 1000 Ljubljana, Slovenia*
[c] *Département de Toxicologie et Risques Chimiques, Institut de Recherche Biomédicale des Armées, 91223 Brétigny sur Orge, France*
[d] *Department of Pharmacy and Pharmaceutical Technology and Physical Chemistry, Faculty of Pharmacy and Food Science, University of Barcelona, Barcelona, Spain*
[e] *Institute of Nanoscience and Nanotechnology (IN2UB), University of Barcelona, Barcelona, Spain*

ARTICLE INFO

Article history:
Received 9 June 2021
Received in revised form
12 August 2021
Accepted 13 August 2021
Available online 19 August 2021

Keywords:
Alzheimer's disease
Multifunctional agents
β-amyloid
Tau protein
Cholinesterase inhibitors
5-HT_6 antagonists

ABSTRACT

Multifunctional ligands as an essential variant of polypharmacology are promising candidates for the treatment of multi-factorial diseases like Alzheimer's disease. Based on clinical evidence and following the paradigm of multifunctional ligands we have rationally designed and synthesized a series of compounds targeting processes involved in the development of the disease. The biological evaluation led to the discovery of two compounds with favorable pharmacological characteristics and ADMET profile. Compounds **17** and **35** are 5-HT_6R antagonists (K_i = 13 nM and K_i = 15 nM respectively) and cholinesterase inhibitors with distinct mechanisms of enzyme inhibition. Compound **17**, a tacrine derivative is a reversible inhibitor of acetyl- and butyrylcholinesterase (IC_{50} = 8 nM and IC_{50} = 24 nM respectively), while compound **35** with rivastigmine-derived phenyl *N*-ethyl-*N*-methylcarbamate fragment is a selective, pseudo-irreversible inhibitor of butyrylcholinesterase (IC_{50} = 455 nM). Both compounds inhibit aggregation of amyloid β *in vitro* (75% for compound **17** and 68% for **35** at 10 μM) moreover, compound **35** is a potent tau aggregation inhibitor *in cellulo* (79%). In ADMET *in vitro* studies both compounds showed acceptable metabolic stability on mouse liver microsomes (28% and 60% for compound **17** and **35** respectively), no or little effect on CYP3A4 and 2D6 up to a concentration of 10 μM and lack of toxicity on HepG2 cell line (IC_{50} values of 80 and 21 μM, for **17** and **35** respectively). Based on the pharmacological characteristics and favorable pharmacokinetic properties, we propose compounds **17** and **35** as an excellent starting point for further optimization and in-depth biological studies.

1. Introduction

The search for novel therapeutic approaches against Alzheimer's disease (AD) is an urgent issue. This is due to the common flaw of available therapies, incapable of stopping or even slowing down the progression of AD, and the still growing number of patients suffering from AD [1,2]. Besides the great economic impact imposed by the care costs of AD patients [2], the disease has a profound humanitarian dimension associated with the suffering of individuals affected by AD and difficulty in providing adequate care.

The exact cause of AD remains ambiguous and a significant amount of data on AD pathomechanism indicates its multifactorial nature [3]. In AD, the normal functioning of the brain is precluded due to neurodegenerative lesions and concomitant abnormal neurotransmission [4]. In the past, the latter was mainly associated with the cholinergic system and led to the development of the first

* Corresponding author.
E-mail address: anna.wieckowska@uj.edu.pl (A. Więckowska).

https://doi.org/10.1016/j.ejmech.2021.113783

pharmacotherapeutics in AD being based on cholinesterase inhibitors (ChEIs), currently including three drugs – donepezil, rivastigmine and galantamine [5–8]. In fact, the abnormal neurotransmission affects not only cholinergic, but also glutamatergic, GABA-ergic and serotonergic neurotransmitter systems [9–11]. The typical AD brain is also a place of accumulation of pathological proteins, such as senile plaques and neurofibrillary tangles (NFTs) [12–14]. Senile (amyloid) plaques are a result of β-amyloid (Aβ) aggregation. Aβ represents a group of peptides which are formed from the amyloid precursor protein (APP) in a series of reactions to form oligomers, fibrils and plaques [15,16]. These species trigger inflammatory responses, contribute to oxidative stress and impair cellular communication, ultimately leading to neuronal injury and cognitive dysfunctions [17–19]. NFTs arise when the tau protein is hyperphosphorylated by tau-kinases, followed by other post-translational modifications such as acetylation [20,21]. This drives the dissociation of tau from the microtubules and initiates aggregation of hyperphosphorylated tau, which similarly to Aβ forms oligomers and ultimately intracellular deposits called the *neurofibrillary tangles* [22]. The hyperphosphorylated tau and the NFTs are linked to impaired long- and short-term synaptic plasticity [22,23].

The complex pathomechanism of AD inclines to search for multifunctional ligands (multi-target-directed ligands, MTDLs) – compounds that are designed to interact with several disease-relevant biological targets [24–26]. Their main advantage in multi-target therapy over co-administration of several active substances involves their simplified pharmacokinetic and pharmacodynamic profile and thus a minimised risk of unwanted and potentially life-threatening drug-drug interactions (DDI) [27]. Currently, MTDLs attract much attention due to their lower development cost when compared with two or more separate drugs, and an increasing number of FDA-approved drugs are multifunctional drugs [28].

Continuing our previous research, herein we report novel multifunctional ligands against AD which combine the inhibitory activity towards cholinesterases with 5-HT_6 receptor (5-HT_6R) antagonism, and anti-aggregation properties against Aβ and tau protein. Although marketed ChEIs cannot stop the progression of the disease [29], anti-cholinesterase activity is a clinically verified approach and therefore it is used in the design of multifunctional ligands [26,30–33]. Of the two cholinesterases: acetylcholinesterase (AChE) and butyrylcholinesterase (BuChE), the latter may for several reasons be regarded as a viable alternative to AChE as a target for AD therapies. Functional equilibrium occurring in the physiological conditions between these enzymes is disrupted in the course of the disease in favor of BuChE [34], therefore it can take over the regulation of acetylcholine levels as shown in studies with AChE and BuChE knockout mice [35,36]. Moreover, a recently developed selective BuChE inhibitor improves memory and learning abilities of mice in a scopolamine-induced cognitive deficit model without producing acute cholinergic adverse effects [37].

In the search for therapies that can modulate the disturbed neurotransmission in AD, the serotonergic system, especially the 5-HT_4 and 5-HT_6 receptors have come in the limelight [38–40]. In particular, research has been focused on 5-HT_4R agonists, 5-HT_6R antagonists and several multifunctional compounds with these activities are found in the literature [41–45]. The rationale behind the use of 5-HT_6R antagonists in AD therapy is a positive effect of 5-HT_6R blockade on cognition [46,47] and a linkage between serotonergic and cholinergic systems. In particular, 5-HT_6R antagonists increase the acetylcholine levels and reverse cognition deficits induced by the administration of anticholinergic agents [48,49]. This effect is mediated by multiple neurotransmitter systems including serotonergic, cholinergic, glutamatergic and GABAergic [50–55] and thus provides beneficial anti-AD activities [50]. The interest in 5-HT_6R antagonists also stems from their pleiotropic activities, involving the alleviation of anxiety or depression symptoms, as shown in preclinical studies [56,57]. In addition, 5-HT_6R antagonists regulate synaptic remodelling [58] and neuronal hyperexcitability [59], which are among plausible causes of AD and point to the potential disease-modifying effect of 5-HT_6R antagonists. The observed improvement of cognitive functions in Phase II clinical trials with the 5-HT_6R antagonists idalopirdine and intepirdine co-administered with ChEI [60,61] further paves the way for the development of multifunctional ligands combining serotoninergic and cholinergic activities.

2. Results and discussion

2.1. Design of compounds

Given the beneficial effects of the combination therapy with a ChEI and 5-HT_6 antagonist demonstrated in clinical trials we have designed compounds combining these two mechanisms in multifunctional ligands (Fig. 1). As cholinesterase-targeting fragments we have used well-known molecular scaffolds - tacrine (1,2,3,4-tetrahydroacridin-9-amine, series I), *N*-benzylamine derived from donepezil and phenyl *N*-ethyl-*N*-methylcarbamate fragment from rivastigmine. These scaffolds have been used extensively in the development of ChEI and multifunctional ligands against AD and we have observed that tacrine fragment is the most effective in terms of cholinesterase inhibition [62–67]. In our previous works [66,67] we have confirmed the efficiency of 1-(phenylsulfonyl)-4-(piperazin-1-yl)-1*H*-indole as a 5-HT_6R-targeting fragment in MTDLs. Here, we replaced piperazine moiety with the oxyethylene fragment that was previously revealed as its bioisostere and linked it with alkyl fragments of different lengths (series I and II). Based on molecular modelling studies, we expected that the higher conformational flexibility of the linker would be beneficial for cholinesterase inhibition allowing benzylamine/tacrine to reach the bottom of the active site gorge and to adopt an optimal position for interactions with the amino acid residues. Further optimizations were focused on benzylamine substitution (series III), primarily to enhance the cholinesterase inhibitory potencies.

2.2. Chemistry

The final compounds were synthesized according to the synthetic routes presented in Schemes 1 and 2. An essential step in the synthesis was the preparation of primary amines **9**–**16** (Scheme 1). Commercially available 4-benzyloxyindole in reaction with benzenesulfonyl chloride in the presence of potassium *tert*-butoxide

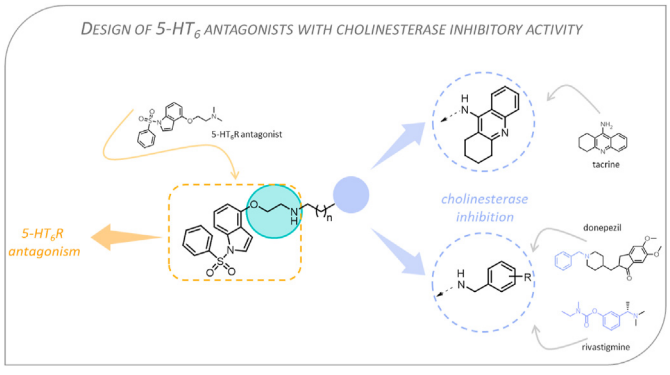

Fig. 1. Design of new multifunctional ligands combining scaffolds with 5-HT_6R antagonism and cholinesterase inhibitory activity.

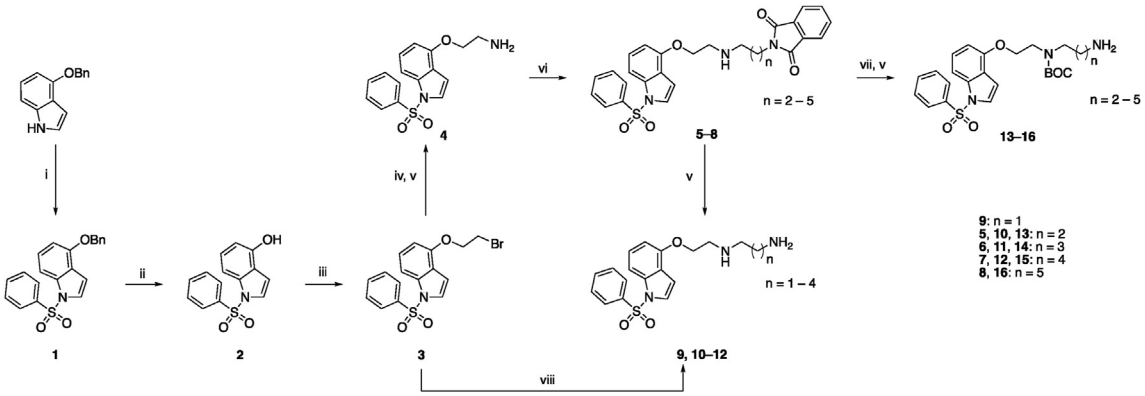

Scheme 1. Synthesis of primary amines **9**–**16**. Reagents and conditions: (i) benzenesulfonyl chloride, potassium *tert*-butoxide, 18-crown-6 ether, THF, 0 °C–rt, 24 h; (ii) 10% Pd/C, $H_{2(g)}$, THF, 45 °C, 2 h; (iii) 1,2-dibromoethane, K_2CO_3, ethanol, reflux, 48 h; (iv) potassium phthalimide, 18-crown-6 ether, DMF, 50 °C, 24 h; (v) CH_3NH_2 (40% aq. sol.), 50 °C, 1 h, then 1 M NaOH, rt, 1 h; (vi) ω-(bromoalkyl)isoindole-1,3-dione, K_2CO_3, MeCN, 100 °C, mw, 1 h; (vii) di-*tert*-butyl dicarbonate, TEA, THF, 0 °C–rt, overnight; (viii) ethylenediamine, MeCN, 80 °C, 2.5 h.

and 18-crown-6 ether, yielded compound **1**. Debenzylation of **1** in the presence of $H_{2(g)}$/Pd/C in tetrahydrofuran (THF) at 45 °C provided the phenol **2**, which was subsequently transformed into 2-bromoethoxy derivative **3** by refluxing with an excess of 1,2-dibromoethane in ethanol, in the presence of K_2CO_3. Primary bromide **3** was used in Gabriel synthesis and transformed into primary amine **4**, which was reacted with ω-(bromoalkyl)isoindole-1,3-diones in acetonitrile (MeCN) at 100 °C under microwave irradiation, yielding compounds **5**–**8**. These compounds were then BOC-protected in the reaction with di-*tert*-butyl dicarbonate and triethylamine (TEA) and phthalimide was subsequently cleaved in a reaction with 40% aqueous solution of methylamine and 1 M NaOH, or directly cleaved without earlier BOC-protection, providing BOC-protected primary amines **13**–**16** or their unprotected counterparts **10**–**12**.

A different approach was used to synthesize ethylenediamine derivative **9**, which was obtained directly from primary bromide **3**, by reacting it with an excess of ethylenediamine in MeCN.

Primary amines **9**–**12** were reacted with the commercially available aldehydes to produce final compounds from **series II** (**22**–**25**) and **series III** (**26**–**35**) (Scheme 2). For the synthesis of **series I** BOC-protected amines **13**–**16** were reacted with 9-chloro-1,2,3,4-tetrahydroacridine (Scheme 2). The reaction required quite harsh conditions – it was conducted in pentan-1-ol under microwave irradiation at 190 °C and this required the use of BOC-protected amines. The cleavage of BOC-group in the presence of 1 M HCl provided final compounds **19**–**21**. In the case of compound **18** a spontaneous BOC-deprotection took place during the microwave-assisted reaction, so the cleavage step was not necessary. Ethylenediamine derivative **17** was obtained from compound **9** in the reaction with 9-chloro-1,2,3,4-tetrahydroacridine in analogous conditions (pentan-1-ol, microwave irradiation, 190 °C) (Scheme 2).

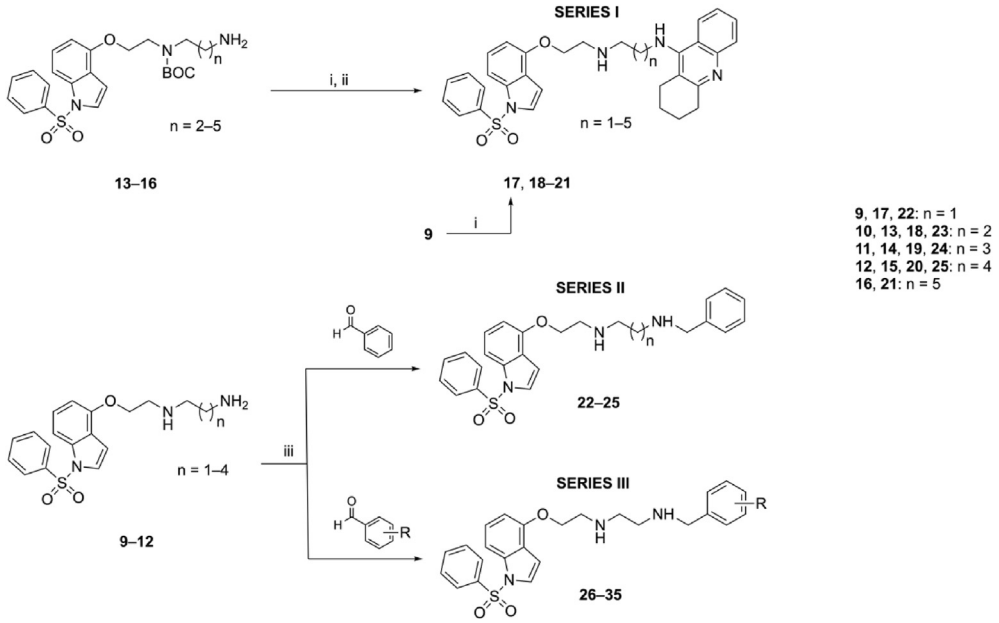

Scheme 2. Synthesis of final compounds. Reagents and conditions: (i) 9-chloro-1,2,3,4-tetrahydroacridine, pentan-1-ol, 190 °C, mw, 2 h; (ii) 1 M HCl in EtOAc, MeOH, rt, overnight; (iii) appropriate aldehyde, CH_3COOH, $NaBH_3CN$, MeOH, 0 °C–rt, 24 h.

2.3. Biological evaluation

2.3.1. Cholinesterase (AChE/BuChE) inhibitory potencies, 5-HT$_6$R binding and functional assays

The inhibitory potency of the compounds from series **I**–**III** against equine serum-derived butyrylcholinesterase (*eq*BuChE) and electric eel-derived acetylcholinesterase (*ee*AChE), was determined using the spectrophotometric method described by Ellman [68]. After the initial screening, at the concentration of 10 μM, IC$_{50}$ values were determined for the compounds with an inhibitory potency higher than 50%. Compounds with less than 50% inhibition against the enzyme were regarded as inactive. Tacrine, donepezil and rivastigmine were used as the positive controls. The affinity of all compounds for the recombinant human 5-HT$_6$ receptor was evaluated in a radioligand binding assay, with methiothepine as a reference [69]. The antagonistic properties of the selected derivatives were confirmed in cell-based functional studies (see Table S1 in the Supporting Information).

The presence of the tacrine moiety in compounds from **series I** ensured high inhibitory activity towards cholinesterases – IC$_{50}$ for *eq*BuChE were in the range of 2–24 nM and 8–303 nM for *ee*AChE (Table 1). With the exception of **17**, all compounds were more potent inhibitors of *eq*BuChE than of *ee*AChE. It is worth emphasizing that we found compounds exceeding the inhibitory potency of tacrine by a factor of 7 (*eq*BuChE IC$_{50}$ of 2 nM for **20** vs. 15 nM for tacrine) and 3 (*ee*AChE IC$_{50}$ of 8 nM for **17** vs. 24 nM for tacrine). This might be due to the additional interactions illustrated in Fig. 2A on the example of compound **17**. The compound is bound in the catalytic site of BuChE in a way common for tacrine-based inhibitors – the heteroaromatic ring forms both π-π and π-cation interactions with Trp82. However, in addition to the tacrine itself, the protonated nitrogen atom from the linker of **17** forms a salt bridge with Asp70 side chain, whereas the 1-(benzenesulfonyl)-1*H*-indole fragment, which is primarily responsible for recognition in the 5-HT$_6$R, found interactions with Phe329 (π-stacking) and Ser198 (hydrogen bond). Structural modifications, namely elongation of the alkyl linker (n = 1–5) had a limited influence on the *eq*BuChE inhibitory potencies and reduced *ee*AChE inhibition. Compounds from **series I** also showed a strong affinity for 5-HT$_6$R, with K_i values in the range of 3.5–13 nM, showing that the potency is not affected by the changing distance between tacrine and 5-HT$_6$-targeting moiety. Docking studies, as exemplified by the predicted binding mode of compound **17** in the 5-HT$_6$R homology model (Fig. 2B) revealed an exemplary binding mode, which was in line with the previously described analogous piperazine derivatives [66]. Compound **17** interacts with Asp3.32^{106} (salt bridge/charge-assisted hydrogen bond) and Phe6.52^{285} (CH-π stacking) – the two main anchoring interactions, conserved in GPCRs for monoamines. The remaining interactions in the orthosteric binding site, CH-π stacking with Phe5.38^{188} and hydrogen bond with Asn6.55^{288} are characteristic solely of 5-HT$_6$R. CH-π stacking interactions with Phe7.35^{302} and a salt bridge with Asp7.36^{303} in the accessory binding site are characteristic of tacrine derivatives.

Replacement of tacrine by benzylamine aimed to reduce the molecular weight of the compounds and to improve the physicochemical properties (**series II**). Unfortunately, this modification led to the loss of activity against *ee*AChE (Table 1) with the exception of compound **22** (IC$_{50}$ = 2869 nM; Table 1). The inhibitory potencies of compounds **22**–**25** against *eq*BuChE ranged from 394 to 887 nM. Structural modifications of the phenyl ring in the benzylamine moiety in compound **22** led to **series III** with *eq*BuChE IC$_{50}$ values ranging from 455 to 4263 nM (Table 1). Interestingly, compound **35** with rivastigmine-derived *N*-ethyl-*N*-methylcarbamate substituent at position 3 of the phenyl ring displayed improved inhibitory activity for *eq*BuChE (IC$_{50}$ = 455 nM). The compound adopted a similar arrangement in the binding site of BuChE to compound **17**, forming analogous interactions. The *N*-ethyl-*N*-methylcarbamate moiety, which is essential for pseudo-irreversible inhibition of cholinesterases by rivastigmine, approached Ser198 at a distance of 5 Å, which suggests possible covalent interaction herein (Fig. 3A).

Although the inhibitory potency against *ee*AChE was preserved in some compounds from **series III** (**26**, **27**, **30** and **33**), it was weaker than **22**. At the same time, in both **series II** and **III**, the high affinities for 5-HT$_6$R were retained with K_i values in a low nanomolar range of 0.1–15 nM. We observed that the presence of a halogen atom (Cl, F) or an electron-withdrawing group such as –NO$_2$ or –CF$_3$ at position 3 or 4 of the phenyl in benzylamine enhanced the 5-HT$_6$R affinity; this effect was particularly pronounced for the 4-fluoro derivative **30** (K_i = 0.1 nM vs 3.0 nM for unsubstituted derivative **22**). Fig. 3B shows the predicted binding mode of compound **35** within 5-HT$_6$R. Compound **35** retained all

Table 1
Affinity for 5-HT$_6$R, inhibition of *eq*BuChE and *ee*AChE by compounds from **series I**–**III**.

Comp.	n	5-HT$_6$R		*eq*BuChE	*ee*AChE
		K_i[a] [nM]	K_b[a] [nM]	IC$_{50}$ [nM][b]	
I	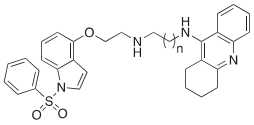				
17	1	13.0 ± 1.4	–	24.39 ± 0.95	8.42 ± 0.07
18	2	10.0 ± 0.6	–	18.76 ± 0.27	20.90 ± 0.52
19	3	3.5 ± 0.5	10 ± 0.5	9.39 ± 0.29	57.54 ± 0.68
20	4	7.0 ± 0.7	–	2.17 ± 0.05	303.1 ± 7.7
21	5	8.6 ± 1.4	–	4.07 ± 0.19	72.48 ± 1.15
II	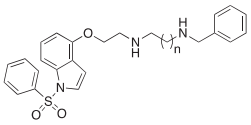				
22	1	3.0 ± 0.2	9 ± 0.4	527.9 ± 7.4	2869 ± 64
23	2	8.0 ± 0.7	–	701.4 ± 11.5	n.a.[c]
24	3	8.0 ± 1.0	–	887.4 ± 20.7	n.a.[c]
25	4	12.0 ± 1.5	–	393.7 ± 8.0	n.a.[c]
III	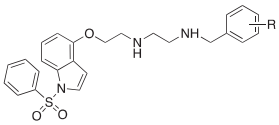				
26	2-Cl	3.0 ± 0.3	58 ± 1.8	585.7 ± 16	4236 ± 73
27	3-Cl	2.0 ± 0.2	–	1075 ± 25	4841 ± 107
28	4-Cl	1.0 ± 0.2	–	1991 ± 92	n.a.[c]
29	3,5-diCl	11.0 ± 1.4	–	1661 ± 75	n.a.[c]
30	4-F	0.1 ± 0.01	–	1304 ± 40	6214 ± 131
31	4-NO$_2$	2.0 ± 0.3	–	4263 ± 135	n.a.[c]
32	4-OMe	3.5 ± 0.3	–	2071 ± 61	n.a.[c]
33	3-Me	2.0 ± 0.2	–	1067 ± 22	4467 ± 97
34	3-CF$_3$	1.7 ± 0.2	7 ± 0.3	2118 ± 102	n.a.[c]
35	3-OCONEtMe	15.0 ± 1.5	48 ± 1.6	454.5 ± 9.0	n.a.[c]
Donepezil		–	–	1830 ± 40	11.00 ± 0.20
Tacrine		–	–	15.00 ± 0.10	23.00 ± 0.40
Rivastigmine		–	–	2195 ± 52	–
Methiothepine		0.30 ± 0.03	–	–	–
SB258585		–	0.36 ± 0.03	–	–

[a] K_i and K_b values are expressed as the mean ± standard error of the mean (SEM) of at least three experiments. [b] IC$_{50}$ values are expressed as the mean ± standard error of the mean (SEM) of at least three experiments; *eq*BuChE from equine serum, *ee*AChE from electric eel. [c] not active.

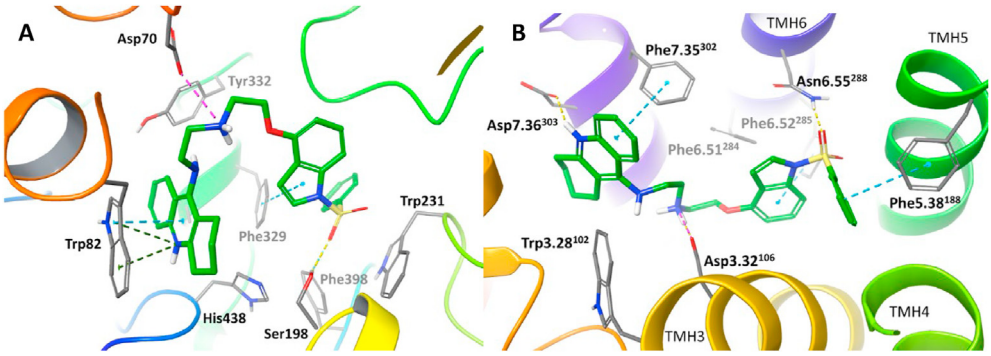

Fig. 2. A) The predicted binding mode of compound **17** within human BuChE catalytic site (PDB ID: 7awg) with typical for tacrine-containing inhibitors interactions with Trp82, supplemented by additional low energy bonds. B) The predicted binding mode of compound **17** in the 5-HT_6R homology model (based on 4IAR [70]), presenting an interaction grid required for ligand recognition. Amino acid residues engaged in ligand binding (within 3 Å from the ligand atoms) are represented as thick sticks. The extracellular loop 2 of the 5-HT_6R was hidden for clarity. TMH – transmembrane helix.

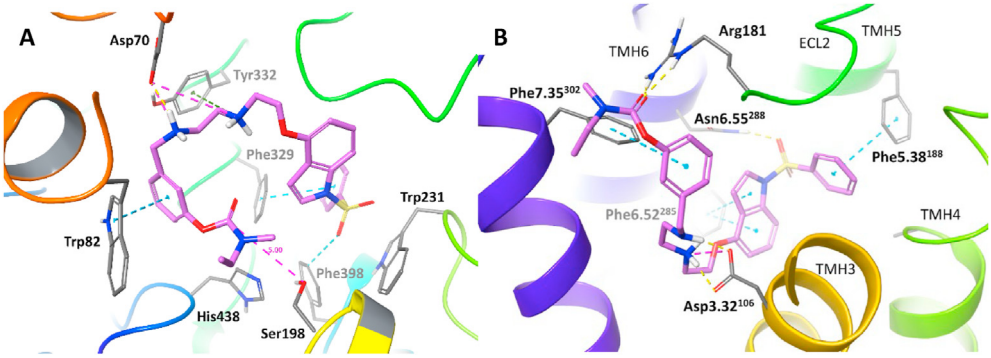

Fig. 3. A) The predicted binding mode of compound **35** within human BuChE catalytic site (PDB ID: 7awg) show close positioning of the *N*-ethyl-*N*-methylcarbamate moiety to catalytic Ser198 (5 Å). B) The predicted binding mode of compound **35** within 5-HT_6R binding site, showing interaction with Arg181characteristic for 5-HT_6R ligands [71]. Amino acid residues engaged in ligand binding (within 3 Å from the ligand atoms) are represented as thick sticks. The extracellular loop 2 (ECL2) of the 5-HT_6R was partially hidden for clarity. TMH – transmembrane helix.

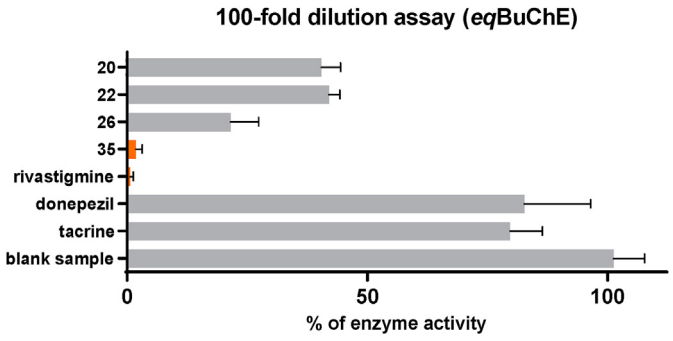

Fig. 4. Results of the 100-fold dilution assay with *eq*BuChE performed for compounds **20**, **22**, **26**, and **35** with rivastigmine, donepezil, and tacrine as references.

the interactions characteristic of 5-HT_6R ligands: salt bridge/charge-assisted hydrogen bond with Asp3.32^{106}, CH-π stackings with Phe6.52^{285} and Phe5.38^{188}, and a hydrogen bond with Asn6.55^{288} in the orthosteric binding site. The tacrine-replacing reduced aromatic moiety preserved the CH-π stacking with Phe7.35^{302} in the accessory binding site. Moreover, the *N*-ethyl-*N*-methylcarbamate substituent formed favourable H-bond interactions with Arg181, a residue from the extracellular loop 2 (ECL2) involved in the 5-HT6R ligand recognition [71].

2.3.2. *Mechanism of BuChE inhibition by selected compounds from series I-III*

The presence of the carbamate moiety in the marketed anti-AD drug rivastigmine is responsible for its pseudo-irreversible inhibition, resulting from the carbamoylation of a serine residue in the catalytic site of ChE. To verify the inhibition mode of the carbamate-based compound **35** we have used the reversibility 100-fold dilution assay described by Kosak et al. [72] For the comparison we have also tested the selected non-carbamate derivatives **20**, **22**, and **26** from **series I-III**. The results indicate that both **35** and rivastigmine, unlike donepezil, tacrine, **20**, **22**, and **26**, inhibit BuChE irreversibly under the assay conditions used (Fig. 4). In the dilution assay, the recovery of BuChE activity was measured after 100-fold dilution of the preincubated mixture of the enzyme with inhibitors. Due to the enzyme carbamoilation pseudo-irreversible inhibitors: **35** and rivastigmine kept BuChE inactive even after dilution, while reversible compounds were not able to completely inhibit enzyme after 100-fold dilution.

2.3.3. *Inhibitory activity against $A\beta_{42}$ and tau*

Compounds that directly inhibit Aβ$_{42}$ and tau aggregation processes attract much attention due to their potential utility as anti-AD therapies. The fact that miscellaneous structures have been shown to possess anti-aggregation properties against Aβ$_{42}$ and tau [73] prompted us to assess these properties of compounds described in this project.

Initially, we have investigated the inhibitory activity of

compounds from **series I**–**III** against $A\beta_{42}$ in an *in vitro* thioflavin T (ThT)-based fluorometric assay in which the benzothiazole dye (ThT) interacts with the cross β-sheet quaternary structure of the amyloid protein. The level of $A\beta_{42}$ aggregation is assessed based on the changes in the fluorescence, which increases when the dye binds to β-sheet structures [74]. The assay was performed at a screening concentration of 10 μM and the results are presented in Tables 2 and 3. Furthermore, we evaluated the anti-aggregation activity against Aβ and tau of the compounds from **series III** in an *in cellulo* assay using the recombinant *Escherichia coli* model. The assay is based on the same principle as the $A\beta_{42}$ *in vitro* thioflavin T (ThT) test, but it is conducted in *vivo* conditions [75]. *Escherichia coli* overexpressing $A\beta_{42}$ or tau serve as the source of proteins, and these are stained by Thioflavin-S (ThS) dye in real-time. Fluorescence changes of ThS in induced and noninduced bacteria cells allow for the calculation of the level of aggregation of $A\beta_{42}$ or tau [76]. The results of the *in cellulo* assays are presented in Table 3.

All compounds from **series I** (Table 2) inhibited β-amyloid aggregation by more than 60% at 10 μM, with 77% inhibition for the most active compound, **19**. The benzylamine analogues from **series II** (Table 2) were slightly weaker inhibitors than their tacrine-bearing counterparts from **series I**, showing potency in the 42%–62% range at 10 μM.

The activity of the compounds from **series III** in an *in vitro* $A\beta_{42}$ assay (Table 3) ranged from 55% to 73%, pointing to a positive effect of the selected substituents on the inhibitory activity when compared to the unsubstituted derivative **22**. Only compound **34** (3-CF_3 substituent), was inactive *in vitro*, but despite this, interestingly, it showed the best performance in the *in cellulo* assay with $A\beta_{42}$ (48% of inhibition at 10 μM). The remaining compounds displayed weaker anti-$A\beta_{42}$ inhibitory activity *in cellulo* than *in vitro* (24–49% at 10 μM). In the *in cellulo* assay using tau protein the compounds showed similar inhibitory potencies ranging from 52%, for the 2-Cl substituted derivative **26**, to 79% for the carbamate **35**. The IC_{50} values were established for the two promising multifunctional ligands: **17** (IC_{50} = 1.10 ± 0.23 μM) and **35** (IC_{50} = 1.38 ± 0.45 μM).

Considering their influence on the aggregation of $A\beta_{42}$ and tau proteins, compounds **30** and **35** are of special interest due to the particularly high and balanced inhibitory potency. Compound **30** with 73% and 41% inhibition of $A\beta_{42}$ aggregation in the *in vitro* and *in cellulo* assays respectively, and 62% tau inhibition, **35**, with inhibition values of 68% and 79% in the $A\beta_{42}$ *in vitro* and tau *in cellulo* assays, respectively.

Table 2
In vitro inhibitory activity against $A\beta_{42}$ for compounds from **series I** and **II**.

Comp.	n	Inhibition of $A\beta_{42}$ aggregation [%][a]/IC_{50} [μM][b]
	I	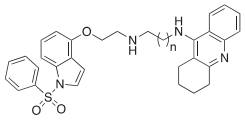
17	1	74.8 ± 7.7/1.10 ± 0.23[b]
18	2	61.1 ± 20.6
19	3	77.4 ± 7.4
20	4	73.2 ± 13.1
21	5	69.2 ± 8.8
	II	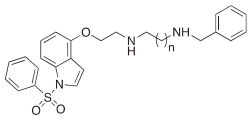
22	1	55.0 ± 12.1
23	2	53.2 ± 1.9
24	3	41.8 ± 5.6
25	4	62.5 ± 1.0
resveratrol		86.6% ± 11.6[c]

[a] Inhibition percentage at 10 μM compound and 1.5 μM $A\beta_{42}$. Inhibition percentage means ± SD from at least two independent experiments, each performed in quadruplicate. Statistical analysis: one-way ANOVA, followed by *post-hoc* Bonferroni *t*-test (SigmaPlot v 12.0), compared to control experiment ($A\beta_{42}$ + DMSO); $p < 0.05$; [b] The IC_{50} values are reported as mean ± SEM of three independent experiments; [c] Ref. Pasieka et al. [77].

2.3.4. Preliminary in vitro ADMET profiling

Based on their favorable profile of *in vitro* activities we selected compounds **17** and **35** for further *in vitro* ADMET profiling studies.

Permeability. We assessed the permeability of compounds **17** and **35** in the Parallel Artificial Membrane Permeability Assay (PAMPA) assay described by Chen et al. using caffeine as well-permeable and norfloxacin as low-permeable references [79]. Based on the permeability coefficient (*Pe*) values obtained we classified compound **35** as permeable (Table 4). According to the results, compound **17** might face some problems with passing the biological membranes (Table 4). We hypothesize that it might result from the high lipophilicity (Table S3 in the Supporting Information) and resulting tendency to retain in the membrane. However, tacrine derivatives that we have previously reported [66,67] not only showed good permeability in PAMPA-BBB but also significant *in vivo* activity, which indirectly confirms the capacity to cross BBB.

Influence on CYP3A4 and CYP2D6 activity. We have used the CYP450 inhibition luminescence assay from Promega as a predictor of the compounds' influence on the metabolism of other drugs that might be co-administered by the patient. The resulting DDIs are an important issue for elderly patients, who are usually on multiple medications. Compounds **17** and **35** showed no or little effect on the two major isoforms of CYP450 – 3A4 and 2D6 up to a concentration of 10 μM (Fig. 5). Considering their biological activity against targets of interest it gives them quite a broad safety margin.

Cytotoxicity on hepatic HepG2 cell line. We have evaluated the influence of compounds **17** and **35** on the viability of human hepatic HepG2 cells in a routinely used MTS assay after 48 h of incubation. This cell line is commonly used in cytotoxicity studies, and considering the hepatotoxic effects caused by tacrine, it was of significant importance for the tacrine-based analogues developed in the study. Up to a concentration of 10 μM, compound **17** did not decrease cell line viability and displayed an IC_{50} value of 79.6 μM, which gives a toxicity index of at least 3000. The IC_{50} determined for **35** was 21.1 μM leaving a much-narrowed safety margin in relation to *eq*BuChE inhibitory activity (see Fig. S4 in the Supporting Information).

Metabolic stability. Liver is a primary site of drug metabolism, therefore, we used mouse liver microsomes (MLM) to determine the metabolic stability of compounds **17** and **35**. The compounds were incubated with MLMs for 2 h and the resulting mixtures were analyzed with UPLC-MS (for details including the UPLC-MS spectra, see Table S2 and Figs. S5–S12 in the Supporting Information). Compound **17** was metabolised in 72% which is similar to verapamil (76%) that was used as a reference while compound **35** in 40%. In line with the predictions by Meta Site software and according to the fragmentation pattern analysis in the UPLC-MS spectra, the major metabolic pathway for both compounds was hydroxylation: in the tacrine fragment for **17**, and in the carbamate moiety for **35**.

3. Conclusions

While tremendous advances have been made in the treatment of many diseases in the last two decades, no drug has been

Table 3
The inhibitory activity of compounds from **series III** towards aggregation processes measured *in vitro* against $A\beta_{42}$ and *in cellulo* against $A\beta_{42}$ and tau.

Comp.	R	Inhibition of aggregation [%]		
		in vitro $A\beta^{a}_{42}$/IC_{50} [μM][c]	*in cellulo* $A\beta^{b}_{42}$	*in cellulo* tau[b]
	III 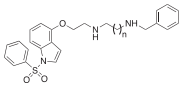			
22	H	55.0 ± 12.1	26.9 ± 1.6	58.1 ± 6.0
26	2-Cl	57.0 ± 10.3	36.5 ± 3.7	51.7 ± 5.4
27	3-Cl	64.3 ± 6.4	27.5 ± 3.5	53.5 ± 2.2
28	4-Cl	60.6 ± 2.3	25.7 ± 0.9	57.5 ± 7.6
29	3,5-diCl	57.2 ± 1.2	31.9 ± 0.4	58.2 ± 4.1
30	4-F	73.4 ± 3.9	40.9 ± 4.5	62.3 ± 5.4
31	4-NO_2	57.7 ± 12.0	23.7 ± 4.3	58.0 ± 5.4
32	4-OMe	63.8 ± 3.3	31.6 ± 4.6	62.3 ± 5.4
33	3-Me	57.4 ± 2.8	41.4 ± 3.6	64.0 ± 6.1
34	3-CF_3	n.i.[d]	48.5 ± 1.3	58.8 ± 2.4
35	3-OCONEtMe	68.1 ± 6.1/1.38 ± 0.45[c]	37.1 ± 6.7	79.4 ± 4.2
resveratrol		86.6 ± 11.6[e]	–	–
DP-128		–	77.5 ± 0.9[f]	68.7 ± 0.5[f]

[a] Inhibition percentage at 10 μM compound and 1.5 μM $A\beta_{42}$. Inhibition percentage means ± SD from at least two independent experiments, each performed in quadruplicate; [b] Inhibition percentage at 10 μM (mean of three experiments ± SEM); [c] The IC_{50} values are reported as mean ± SEM of three independent experiments; [d] No inhibition (percentage lower than 20%). Statistical analysis: one-way ANOVA, followed by *post-hoc* Bonferroni *t*-test (SigmaPlot v 12.0), compared to control experiment ($A\beta_{42}$ + DMSO); $p < 0.05$. [e] Ref. Pasieka et al. [77] [f] Ref. di Pietro et al. [78].

Table 4
The permeability coefficient (*Pe*) values determined for compounds **17**, **35** and references (caffeine as well-permeable and norfloxacin as low-permeable) by PAMPA assay (pre-coated PAMPA Plate System Gentest™, Corning, Tewksbury, MA, USA). For UPLC chromatograms see Figs. S1–S3 in the Supporting Information). [a]Data is expressed as a mean of three replicates (n = 3) ± SD (10^{-6} cm/s).

Compound	*Pe*[a]	CNS (±)
caffeine	7.89 ± 1.12	+
norfloxacin	0.056 ± 0.01	+
17	not calculable	–
35	1.27 ± 0.33	+

approved for the treatment of Alzheimer's disease during this time. Nonetheless, a significant progress has been made in understanding the complexity of AD and multiplicity of processes involved in its development and, consequently, the necessity to use complex therapy. In the meantime, a new paradigm of drug discovery emerged – *multiple ligands* (multitarget-directed ligands, MTDLs or multifunctional ligands) which led to the development of a broad range of new compounds combining biological activities that address the processes important for the disease pathomechanism.

In this paper, we report novel MTDLs incorporating complementary mechanisms grounded in clinical evidence: inhibition of ChE, blockade of 5-HT_6R and inhibition of Aβ and tau aggregation. We have combined pharmacophores addressing 5-HT_6R (2-((1-(phenylsulfonyl)-1*H*-indol-4-yl)oxy)ethan-1-amine) and ChE (tacrine, *N*-benzylamine or phenyl *N*-ethyl-*N*-methylcarbamate), and applied modifications verifying the optimal length of a linker and substituents providing favorable interactions.

Based on the biological evaluation, we identified two compounds that we believe deserve special attention: compound **17** and **35**. Compound **17** is a tacrine-based ligand with balanced activities towards 5-HT_6R (K_i = 13 nM), *ee*AChE (IC_{50} = 8 nM) and *eq*BuChE (IC_{50} = 24 nM) and with inhibitory potency against Aβ aggregation of 75%. Despite the presence of tacrine moiety, compound **17** did not show toxicity on HepG2 cells up to the concentration of 10 μM which gives it a broad safety margin. It also showed no or little influence on the activity of CYP3A4 and 2D6, which is a good prediction for the lack of drug-drug interactions, and it has acceptable metabolic stability in MLMs, comparable to verapamil. According to the PAMPA assay, compound **17** might have problems with membrane permeability and it might need attention in further studies.

Compound **35** contains rivastigmine-derived phenyl *N*-ethyl-*N*-methylcarbamate fragment, which as we proved, determines the pseudo-irreversible mode of action. Its inhibitory potency against *eq*BuChE is higher than rivastigmine's (IC_{50} of 455 nM vs 2195 nM) and it has a high affinity for 5-HT_6R (K_i = 15 nM). Compound **35** displays impressive anti-aggregation properties at 10 μM with 79% inhibition of tau aggregation, and 37% and 68% of inhibition of Aβ aggregation *in cellulo* and *in vitro* respectively. It has a good metabolic stability (40% metabolized after 2 h) and it is membrane-permeable according to the PAMPA assay. Similarly to compound **17** it shows no or little influence on CYP isoenzymes 3A4 and 2D6 activity up to 10 μM and displays IC_{50} of 21 μM in MTS test on HepG2 cell line.

Summing up, the research described herein allowed for the identification of novel multifunctional ligands with balanced activities against 5-HT_6R and ChEs displaying antiaggregation properties. We regard compounds **17** and **35** as promising candidates for broader studies and an excellent starting point for further optimization, due to their promising *in vitro* biological activities and ADMET profile.

4. Experimental section

4.1. Chemistry

4.1.1. General procedures

All reagents were purchased from commercial suppliers and were used without further purification unless stated otherwise. Tetrahydrofuran (THF) and dichloromethane (DCM) were distilled under nitrogen immediately before use. The drying agent used for THF was sodium/benzophenone ketyl, and for DCM, calcium hydride. Microwave reactions were performed in a Discover LabMate (CEM Corporation). Reactions were monitored by thin-layer chromatography carried out on aluminium sheets precoated with silica gel 60 F_{254} (Merck). Compounds were visualized with UV light and

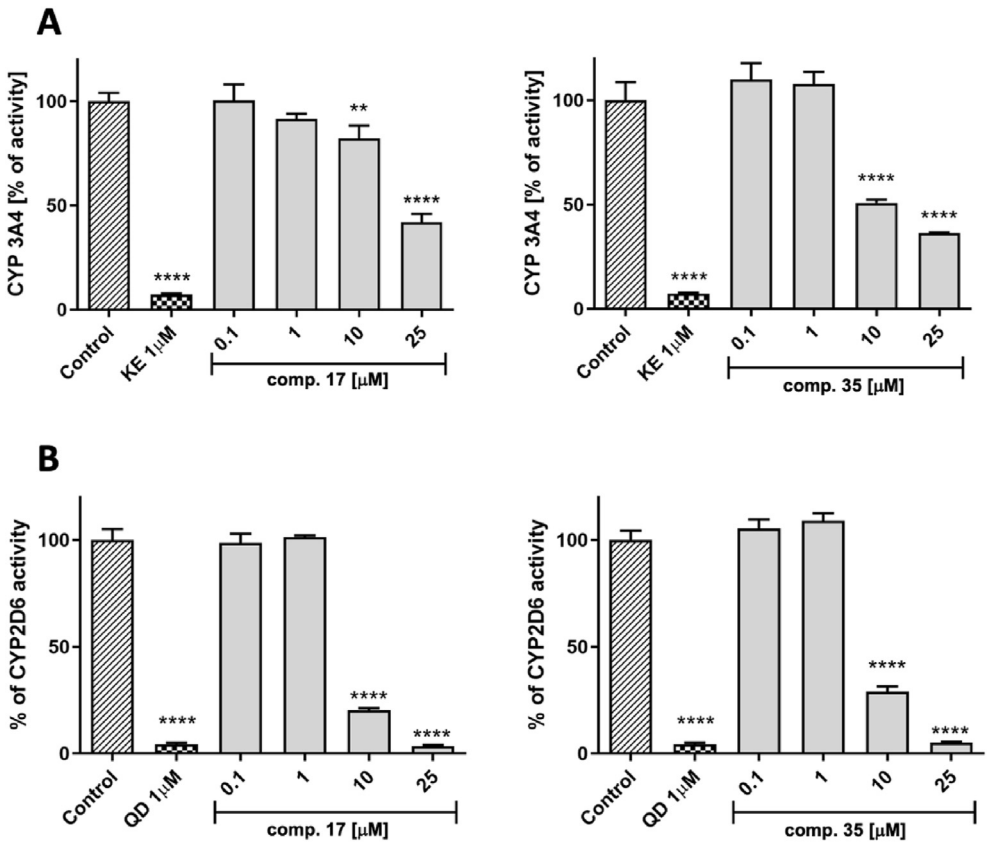

Fig. 5. The influence of increasing concentrations of compounds **17** and **35** (0.1, 1, 10 and 25 μM) and references (KE, ketoconazole; QD, quinidine) on CYP3A4 (**A**) and CYP2D6 (**B**) activity. Statistical significance was evaluated by one-way ANOVA with *post-hoc* Bonferroni test (**p < 0.01, ****p < 0.0001).

by suitable visualization reagents (solution of ninhydrin). Compounds were purified with flash chromatography on Isolera™ Spectra (Biotage) with silica gel 60 (63–200 μm; Merck) as a stationary phase. Analytical RPLC-MS was performed by tandem quadrupole mass spectrometry (Waters Acquity TQD), with detection by UV using a diode array detector with a UPLC BEH C18 column (1.7 μm, 2.1 × 100 mm; Acquity). An MeCN/H_2O gradient with 0.1% HCOOH was used as the mobile phase, at a flow rate of 0.3 mL/min ^{1}H NMR and ^{13}C NMR spectra were recorded on Varian Mercury 300 MHz (Varian, Inc., Palo Alto, CA) or Jeol 500 MHz (Jeol Inc., Peabody, MA). The chemical shifts are reported in ppm and were referenced to the residual solvent signals ($CDCl_3$ ^{1}H: 7.26 ppm, ^{13}C: 77.16 ppm; CD_3OD ^{1}H: 3.31 ppm, ^{13}C: 49.00 ppm), coupling constants are reported in hertz (Hz). Purities of the final compounds were determined using analytical RPLC-MS (Waters Acquity TQD) with a UPLC BEH C18 column (1.7 μm, 2.1 × 100 mm, Aquity), with detection set to 214 nm and 254 nm. An MeCN/H_2O gradient with 0.1% HCOOH was used as the mobile phase, at a flow rate of 0.3 mL/min. The target compounds showed purities of >95% and these are given for each compound in the following description. HRMS analyses were performed on MALDI-TOF/TOF mass spectrometer UltrafleXtreme from Bruker Daltonics (Bremen, Germany) with α-cyano-4-hydroxycinnamic acid (CHCA) MALDI matrix after standard dried droplet preparation on ground steel target plate.

Previously reported compounds.

4-(Benzyloxy)-1-(phenylsulfonyl)-1*H*-indole (**1**) [80], 1-(phenylsulfonyl)-1*H*-indol-4-ol (**2**) [81], 2-((1-(phenylsulfonyl)-1*H*-indol-4-yl)oxy)ethan-1-amine (**4**) [82].

*4.1.2. Synthesis of 4-(benzyloxy)-1-(phenylsulfonyl)-1H-indole (**1**)*

To an ice-bath solution of potassium *tert*-butoxide (3.02 g, 26.9 mmol, 1.2 equiv.) and 18-crown-6 ether (1.18 g, 4.48 mmol, 0.2 equiv.) in 150 mL THF, 4-(benzyloxy)-1*H*-indole (5.00 g, 22.4 mmol, 1 equiv.) dissolved in 65 mL THF was added dropwise; after 30 min, benzenesulfonyl chloride (4.31 mL, 33.6 mmol, 1.5 equiv.) was added and the mixture was stirred at ambient temperature for 18 h. After that time, the solvent was removed in vacuo, the residue was dissolved in DCM, washed with water and brine, dried over Na_2SO_4 and concentrated in vacuo. The crude product was purified by crystallization (chloroform/methanol). Yield: 7.14 g (81%), white solid. ^{1}H NMR (300 MHz, $CDCl_3$) δ 7.85–7.91 (m, 2H), 7.62 (d, J = 8.46 Hz, 1H), 7.50–7.56 (m, 1H), 7.48 (d, J = 3.59 Hz, 1H), 7.29–7.47 (m, 7H), 7.22 (t, J = 8.21 Hz, 1H), 6.84 (dd, J = 0.77, 3.85 Hz, 1H), 6.72 (d, J = 7.95 Hz, 1H), 5.15 (s, 2H). Formula: $C_{21}H_{17}NO_3S$; MS: *m/z* 364 ($M + H^+$).

*4.1.3. Synthesis of 1-(phenylsulfonyl)-1H-indol-4-ol (**2**)*

To 4-(benzyloxy)-1-(phenylsulfonyl)-1*H*-indole (**1**) (7.137 g, 19.6 mmol) dissolved in 150 mL THF 10% Pd/C (2.600 g, 36% w/w) was added and the resulting mixture was hydrogenated at 45 °C for 3 h. Then, the solution was filtered through Celite® and concentrated in vacuo. The resulting solid was used in further steps without purification. Yield: 5.357 g (100%), white solid. ^{1}H NMR (300 MHz, $CDCl_3$) δ 7.85–7.90 (m, 2H), 7.39–7.60 (m, 5H), 7.14 (t, J = 8.08 Hz, 1H), 6.76 (dd, J = 0.77, 3.59 Hz, 1H), 6.62 (dd, J = 0.77, 7.95 Hz, 1H), 5.47 (s, 1H). Formula: $C_{14}H_{11}NO_3S$; MS: *m/z* 274 ($M + H^+$).

*4.1.4. Synthesis of 4-(2-bromoethoxy)-1-(phenylsulfonyl)-1H-indole (**3**)*

The mixture of 1-(phenylsulfonyl)-1*H*-indol-4-ol (**2**) (5.439 g, 19.9 mmol, 1 equiv.), 1,2-dibromoethane (8.574 mL, 99.5 mmol, 5 equiv.) and K_2CO_3 (8.251 g, 59.7 mmol, 3 equiv.) in 150 mL EtOH was stirred at 80 °C for 48 h. After that time, the mixture was filtered, concentrated in vacuo and purified using flash chromatography (0–50% EtOAc in petroleum ether). Yield: 4.762 g (63%), white solid. ^{1}H NMR (500 MHz, $CDCl_3$) δ 7.84–7.88 (m, 2H), 7.63 (d, J = 8.59 Hz, 1H), 7.50–7.54 (m, 1H), 7.48 (d, J = 4.01 Hz, 1H), 7.39–7.44 (m, 2H), 7.21 (t, J = 8.02 Hz, 1H), 6.79–6.82 (m, 1H), 6.62 (d, J = 8.02 Hz, 1H), 4.36 (t, J = 6.30 Hz, 2H), 3.63–3.68 (m, 2H). Formula: $C_{16}H_{14}BrNO_3S$; MS: *m/z* 380 ($M + H^+$).

*4.1.5. Synthesis of 2-(2-((1-(phenylsulfonyl)-1H-indol-4-yl)oxy)ethyl)isoindoline-1,3-dione (**3a**)*

A mixture of an 4-(2-bromoethoxy)-1-(phenylsulfonyl)-1*H*-indole (**3**) (3.705 g, 9.74 mmol, 1 equiv.), potassium phthalimide salt (1.912 g 10.32 mmol, 1.06 equiv.) and 18-crown-6 ether (77 mg, 6.29 mmol, 0.03 equiv.) in 60 mL DMF was stirred at 50 °C for 24 h. After that time, the solvent was removed in vacuo, the residue was dissolved in DCM, washed with water and brine, dried over Na_2SO_4 and concentrated in vacuo. A crude product was purified by crystallization (EtOAc). Yield: 3.686 g (85%), white solid. ^{1}H NMR (300 MHz, $CDCl_3$) δ 7.80–7.86 (m, 4H), 7.68–7.72 (m, 2H), 7.56 (d, J = 8.46 Hz, 1H), 7.46–7.52 (m, 1H), 7.35–7.43 (m, 3H), 7.17 (t, J = 8.08 Hz, 1H), 6.72 (dd, J = 0.77, 3.85 Hz, 1H), 6.60 (d, J = 7.69 Hz, 1H), 4.27 (t, J = 5.13 Hz, 2H), 4.15 (t, J = 5.39 Hz, 2H). Formula: $C_{24}H_{18}N_2O_5S$; MS: *m/z* 447 ($M + H^+$).

*4.1.6. Synthesis of 2-((1-(phenylsulfonyl)-1H-indol-4-yl)oxy)ethan-1-amine (**4**)*

A mixture of 2-(2-((1-(phenylsulfonyl)-1*H*-indol-4-yl)oxy)ethyl)isoindoline-1,3-dione (**3a**) (3.686 g, 8.26 mmol) and 40% aqueous solution of CH_3NH_2 (80 mL) was stirred at 50 °C for 2.5 h. After that time, the mixture was cooled to ambient temperature, 1 M $NaOH_{(aq)}$ was added (80 mL) and the mixture was stirred for 1 h. Next, the mixture was extracted with DCM, combined organic fractions were washed with brine, dried over Na_2SO_4 and concentrated in vacuo. The product was used without further purification. Yield: 2.613 g (100%), brownish solid. ^{1}H NMR (300 MHz, $CDCl_3$) δ 7.80–7.87 (m, 2H), 7.57–7.62 (m, 1H), 7.33–7.51 (m, 4H), 7.17 (t, J = 7.91 Hz, 1H), 6.82 (d, J = 3.52 Hz, 1H), 6.56 (d, J = 8.21 Hz, 1H), 5.39 (br. s., 3H, $-NH_3^+$), 4.05 (t, J = 4.98 Hz, 2H), 3.14 (t, J = 4.98 Hz, 2H). Formula: $C_{16}H_{16}N_2O_3S$; MS: *m/z* 317 ($M + H^+$).

*4.1.7. Synthesis of N^1-(2-((1-(phenylsulfonyl)-1H-indol-4-yl)oxy)ethyl)ethane-1,2-diamine (**9**)*

A mixture of 4-(2-bromoethoxy)-1-(phenylsulfonyl)-1*H*-indole (**3**) (342 mg, 0.90 mmol, 1 equiv.) and ethylenediamine (1023 μL, 15.30 mmmol, 17 equiv.) in 30 mL MeCN was stirred at 80 °C for 2.5 h. After that time, the mixture was cooled to ambient temperature, mixed with 30 mL EtOAc, washed with water and brine, dried over Na_2SO_4 and concentrated in vacuo. The product was purified using flash chromatography (DCM/MeOH/$NH_{3(aq)}$ 90:10:0.5). Yield: 268 mg (83%), yellowish solid. ^{1}H NMR (300 MHz, $CDCl_3$) δ 7.82–7.90 (m, 2H), 7.59 (d, J = 8.21 Hz, 1H), 7.48–7.55 (m, 1H), 7.46 (d, J = 3.52 Hz, 1H), 7.37–7.45 (m, 2H), 7.21 (t, J = 8.21 Hz, 1H), 6.78 (d, J = 3.52 Hz, 1H), 6.65 (d, J = 8.21 Hz, 1H), 4.16 (t, J = 5.27 Hz, 2H), 3.05 (t, J = 5.27 Hz, 2H), 2.71–2.85 (m, 4H), 1.68 (s, 3H). Formula: $C_{18}H_{21}N_3O_3S$; MS: *m/z* 360 ($M + H^+$).

4.1.8. General procedure for the synthesis of compounds 5–8 (GP1)

A 5 mL microwave-transparent vial was charged with the appropriate ω-(bromoalkyl)isoindole-1,3-dione (1 equiv.), 2-((1-(phenylsulfonyl)-1*H*-indol-4-yl)oxy)ethan-1-amine (**4**) (1 equiv.), K_2CO_3 (1.2 equiv.) and MeCN. The vial was capped and exposed to microwave heating at 100 °C for 60 min. After the mixture was cooled to room temperature, acetonitrile was removed, the residue was treated with saturated solution of $NaHCO_{3(aq)}$ and extracted with DCM. Combined organic fractions were washed with brine, dried over Na_2SO_4 and concentrated in vacuo. The crude product was purified by flash chromatography (5% MeOH in DCM).

*4.1.8.1. 2-(3-((2-((1-(Phenylsulfonyl)-1H-indol-4-yl)oxy)ethyl)amino)propyl)isoindoline-1,3-dione (**5**).* Following GP1, compound **5** was prepared using 2-((1-(phenylsulfonyl)-1*H*-indol-4-yl)oxy)ethan-1-amine (**4**) (150 mg, 0.47 mmol), 2-(3-bromopropyl)isoindoline-1,3-dione (126 mg, 0.47 mmol), K_2CO_3 (77 mg, 0.56 mmol) in 3 mL MeCN. Yield: 130 mg (55%), yellowish solid. ^{1}H NMR (300 MHz, $CDCl_3$) δ 7.83–7.89 (m, 2H), 7.75–7.82 (m, 2H), 7.62–7.70 (m, 2H), 7.58 (d, J = 8.21 Hz, 1H), 7.48–7.55 (m, 1H), 7.37–7.47 (m, 3H), 7.19 (t, J = 8.21 Hz, 1H), 6.83 (d, J = 3.52 Hz, 1H), 6.62 (d, J = 8.21 Hz, 1H), 4.11 (t, J = 5.27 Hz, 2H), 3.78 (t, J = 6.74 Hz, 2H), 3.01 (t, J = 5.27 Hz, 2H), 2.73 (t, J = 6.74 Hz, 2H), 1.89 (quin, J = 6.74 Hz, 2H), 1.77 (s, 1H). Formula: $C_{27}H_{25}N_3O_5S$; MS: *m/z* 504 ($M + H^+$).

*4.1.8.2. 2-(4-((2-((1-(Phenylsulfonyl)-1H-indol-4-yl)oxy)ethyl)amino)butyl)isoindoline-1,3-dione (**6**).* Following GP1, compound **6** was prepared using 2-((1-(phenylsulfonyl)-1*H*-indol-4-yl)oxy)ethan-1-amine (**4**) (200 mg, 0.63 mmol), 2-(4-bromobutyl)isoindoline-1,3-dione (177 mg, 0.63 mmol), K_2CO_3 (105 mg, 0.76 mmol) in 3 mL MeCN. Yield: 162 mg (50%), yellowish solid. ^{1}H NMR (300 MHz, $CDCl_3$) δ 7.78–7.89 (m, 4H), 7.66–7.74 (m, 2H), 7.58 (d, J = 8.21 Hz, 1H), 7.38–7.55 (m, 4H), 7.20 (t, J = 7.91 Hz, 1H), 6.79 (d, J = 2.93 Hz, 1H), 6.63 (d, J = 7.62 Hz, 1H), 4.14 (t, J = 5.28 Hz, 2H), 3.70 (t, J = 7.03 Hz, 2H), 3.03 (t, J = 5.27 Hz, 2H), 2.73 (t, J = 7.03 Hz, 2H), 2.16 (br. s., 1H), 1.68–1.80 (m, 2H), 1.50–1.62 (m, 2H).

Formula: $C_{28}H_{27}N_3O_5S$; MS: *m/z* 518 ($M + H^+$).

*4.1.8.3. 2-(5-((2-((1-(Phenylsulfonyl)-1H-indol-4-yl)oxy)ethyl)amino)pentyl)isoindoline-1,3-dione (**7**).* Following GP1, compound **7** was prepared using 2-((1-(phenylsulfonyl)-1*H*-indol-4-yl)oxy)ethan-1-amine (**4**) (200 mg, 0.63 mmol), 2-(5-bromopentyl)isoindoline-1,3-dione (187 mg, 0.63 mmol), K_2CO_3 (105 mg, 0.76 mmol) in 3.5 mL MeCN. Yield: 159 mg (47%), white solid. ^{1}H NMR (300 MHz, $CDCl_3$) δ 7.78–7.88 (m, 4H), 7.65–7.72 (m, 2H), 7.59 (d, J = 8.21 Hz, 1H), 7.37–7.55 (m, 4H), 7.19 (t, J = 8.21 Hz, 1H), 6.78–6.81 (m, 1H), 6.62 (d, J = 7.62 Hz, 1H), 4.17 (t, J = 5.27 Hz, 2H), 3.66 (t, J = 7.03 Hz, 2H), 3.08 (t, J = 5.27 Hz, 2H), 2.69–2.78 (m, 2H), 1.89 (s, 1H), 1.54–1.74 (m, 4H), 1.34–1.40 (m, 2H). Formula: $C_{29}H_{29}N_3O_5S$; MS: *m/z* 532 ($M + H^+$).

*4.1.8.4. 2-(6-((2-((1-(Phenylsulfonyl)-1H-indol-4-yl)oxy)ethyl)amino)hexyl)isoindoline-1,3-dione (**8**).* Following GP1, compound **8** was prepared using 2-((1-(phenylsulfonyl)-1*H*-indol-4-yl)oxy)ethan-1-amine (**4**) (200 mg, 0.63 mmol), 2-(6-bromohexyl)isoindoline-1,3-dione (195 mg, 0.63 mmol), K_2CO_3 (105 mg, 0.76 mmol) in 3.5 mL MeCN. Yield: 83 mg (24%), white solid. ^{1}H NMR (300 MHz, $CDCl_3$) δ 7.79–7.89 (m, 4H), 7.66–7.74 (m, 2H), 7.59 (d, J = 8.79 Hz, 1H), 7.37–7.55 (m, 4H), 7.20 (t, J = 8.21 Hz, 1H), 6.79 (d, J = 3.52 Hz, 1H), 6.63 (d, J = 7.62 Hz, 1H), 4.16 (t, J = 4.98 Hz, 2H), 3.66 (t, J = 7.33 Hz, 2H), 3.05 (t, J = 4.98 Hz, 2H), 2.62–2.75 (m, 4H), 1.67 (quin, J = 7.18 Hz, 2H), 1.46–1.59 (m, 2H), 1.31–1.40 (m, 3H). Formula: $C_{30}H_{31}N_3O_5S$; MS: *m/z* 546 ($M + H^+$).

4.1.9. General procedure for the synthesis of compounds 13–16 (GP2)

Compounds **13**–**16** were prepared in two-step synthesis. *Step 1*. To a solution of secondary amine **5**–**8** (1 equiv.) and TEA (3 equiv.)

in 2 mL of anhydrous THF cooled on an ice-bath, di-*tert*-butyl dicarbonate (1.1–1.2 equiv.) solution in 2 mL anhydrous THF was added dropwise. The reaction was stirred overnight at room temperature and then the solvent was removed in vacuo. The resulting residue was treated with saturated solution of $NaHCO_{3(aq)}$ and extracted with DCM. Combined organic fractions were washed with brine, dried over Na_2SO_4 and concentrated in vacuo. The crude product was purified by flash chromatography (20–55% EtOAc in petroleum ether). *Step 2*. A mixture of the product from Step 1 and 40% aqueous solution of CH_3NH_2 (10 mL for 1 mmol of a compound) was stirred at 50 °C for 2.5 h. After that time, the mixture was cooled to ambient temperature, 1 M $NaOH_{(aq)}$ was added (10 mL for 1 mmol of a compound) and the mixture was stirred for 1 h. Next, the mixture was extracted with DCM, combined organic fractions were washed with brine, dried over Na_2SO_4 and concentrated in vacuo. The crude product used in further steps without purification.

*4.1.9.1. Tert-butyl (3-aminopropyl)(2-((1-(phenylsulfonyl)-1H-indol-4-yl)oxy)ethyl)carbamate (**13**).* Compound **13** was prepared following **GP2**. *Step 1*. 2-(3-((2-((1-(Phenylsulfonyl)-1*H*-indol-4-yl)oxy)ethyl)amino)propyl)isoindoline-1,3-dione (**5**) (155 mg, 0.31 mmol, 1 equiv.), TEA (130 μL, 0.93 mmol, 3 equiv.), di-*tert*-butyl dicarbonate (74 mg, 0.34 mmol, 1.1 equiv.) in 4 mL dry THF. Yield: 148 mg (79%), white solid. Formula: $C_{32}H_{33}N_3O_7S$; MS: *m/z* 604 ($M + H^+$). *Step 2*. Product from Step 1 (148 mg, 0.25 mmol), 40% aqueous solution of CH_3NH_2 (2.5 mL), 1 M $NaOH_{(aq)}$ (2.5 mL). Yield: 95 g (80%). Formula: $C_{24}H_{31}N_3O_5S$; MS: *m/z* 474 ($M + H^+$).

*4.1.9.2. Tert-butyl (4-aminobutyl)(2-((1-(phenylsulfonyl)-1H-indol-4-yl)oxy)ethyl)carbamate (**14**).* Compound **14** was prepared following **GP2**. *Step 1*. 2-(4-((2-((1-(Phenylsulfonyl)-1*H*-indol-4-yl)oxy)ethyl)amino)butyl)isoindoline-1,3-dione (**6**) (162 mg, 0.31 mmol, 1 equiv.), TEA (130 μL, 0.93 mmol, 3 equiv.), di-*tert*-butyl dicarbonate (74 mg, 0.34 mmol, 1.1 equiv.) in 4 mL dry THF. Yield: 191 mg (100%), white solid. Formula: $C_{33}H_{35}N_3O_7S$; MS: *m/z* 618 ($M + H^+$). *Step 2*. Product from Step 1 (191 mg, 0.31 mmol), 40% aqueous solution of CH_3NH_2 (3.1 mL), 1 M $NaOH_{(aq)}$ (3.1 mL). Yield: 140 mg (93%). Formula: $C_{25}H_{33}N_3O_5S$; MS: *m/z* 488 ($M + H^+$).

*4.1.9.3. Tert-butyl (5-aminopentyl)(2-((1-(phenylsulfonyl)-1H-indol-4-yl)oxy)ethyl)carbamate (**15**).* Compound **15** was prepared following **GP2**. *Step 1*. 2-(5-((2-((1-(Phenylsulfonyl)-1*H*-indol-4-yl)oxy)ethyl)amino)pentyl)isoindoline-1,3-dione (**7**) (155 mg, 0.29 mmol, 1 equiv.), TEA (121 μL, 0.87 mmol, 3 equiv.), di-*tert*-butyl dicarbonate (76 mg, 0.35 mmol, 1.2 equiv.) in 4 mL dry THF. Yield: 160 mg (82%), white solid. ^{1}H NMR (300 MHz, $CDCl_3$) δ 7.86–7.89 (m, 1H), 7.80–7.86 (m, 3H), 7.67–7.75 (m, 2H), 7.58 (d, J = 8.21 Hz, 1H), 7.37–7.55 (m, 4H), 7.20 (t, J = 8.21 Hz, 1H), 6.72 (d, J = 3.52 Hz, 1H), 6.63 (d, J = 8.21 Hz, 1H), 4.14–4.19 (m, 2H), 3.60 (br. s., 2H), 3.29 (t, J = 6.74 Hz, 2H), 1.53–1.77 (m, 6H), 1.41 (br. s., 9H), 1.29–1.36 (m, 2H). Formula: $C_{34}H_{37}N_3O_7S$; MS: *m/z* 632 ($M + H^+$). *Step 2*. Product from Step 1 (158 mg, 0.25 mmol), 40% aqueous solution of CH_3NH_2 (2.5 mL), 1 M $NaOH_{(aq)}$ (2.5 mL). Yield: 116 mg (92%). Formula: $C_{26}H_{35}N_3O_5S$; MS: *m/z* 502 ($M + H^+$).

*4.1.9.4. Tert-butyl (6-aminohexyl)(2-((1-(phenylsulfonyl)-1H-indol-4-yl)oxy)ethyl)carbamate (**16**).* Compound **16** was prepared following **GP2**. *Step 1*. 2-(6-((2-((1-(Phenylsulfonyl)-1*H*-indol-4-yl)oxy)ethyl)amino)hexyl)isoindoline-1,3-dione (**8**) (93 mg, 0.17 mmol, 1 equiv.), TEA (72 μL, 0.51 mmol, 3 equiv.), di-*tert*-butyl dicarbonate (41 mg, 0.19 mmol, 1.1 equiv.) in 2 mL dry THF. Yield: 105 mg (96%), white solid. Formula: $C_{35}H_{39}N_3O_7S$; MS: *m/z* 646 ($M + H^+$). *Step 2*. Product from Step 1 (105 mg, 0.16 mmol), 40% aqueous solution of CH_3NH_2 (1.6 mL), 1 M $NaOH_{(aq)}$ (1.6 mL). Yield: 73 mg (88%). Formula: $C_{27}H_{37}N_3O_5S$; MS: *m/z* 516 ($M + H^+$).

4.1.10. General procedure for the synthesis of compounds 10–12 (GP3)

A mixture of phthalimide derivative (**5**–**7**) and 40% aqueous solution of CH_3NH_2 (10 mL for 1 mmol of a compound) was stirred at 50 °C for 2.5 h. After that time, the mixture was cooled to ambient temperature, 1 M $NaOH_{(aq)}$ was added (10 mL for 1 mmol of a compound) and the mixture was stirred for 1 h. Next, the mixture was extracted with DCM, combined organic fractions were washed with brine, dried over Na_2SO_4 and concentrated in vacuo. The crude product was used in further steps without purification.

*4.1.10.1. N^1-(2-((1-(Phenylsulfonyl)-1H-indol-4-yl)oxy)ethyl)propane-1,3-diamine (**10**).* Following **GP3**, compound **10** was prepared using 2-(3-((2-((1-(phenylsulfonyl)-1*H*-indol-4-yl)oxy)ethyl)amino)propyl)isoindoline-1,3-dione (**5**) (130 mg, 0.26 mmol), 40% aqueous solution of CH_3NH_2 (2.6 mL), 1 M $NaOH_{(aq)}$ (2.6 mL). The product was used without further purification. Yield: 77 mg (79%), yellowish oil. ^{1}H NMR (300 MHz, $CDCl_3$) δ 7.84–7.89 (m, 2H), 7.60 (d, J = 8.21 Hz, 1H), 7.39–7.56 (m, 4H), 7.21 (t, J = 8.21 Hz, 1H), 6.76–6.79 (m, 1H), 6.65 (d, J = 8.21 Hz, 1H), 4.16 (t, J = 4.98 Hz, 2H), 3.04 (t, J = 5.27 Hz, 2H), 2.72–2.81 (m, 4H), 1.65 (quin, J = 6.89 Hz, 2H), 1.48 (s, 3H). Formula: $C_{19}H_{23}N_3O_3S$; MS: *m/z* 374 ($M + H^+$).

*4.1.10.2. N^1-(2-((1-(Phenylsulfonyl)-1H-indol-4-yl)oxy)ethyl)butane-1,4-diamine (**11**).* Following **GP3**, compound **11** was prepared using 2-(4-((2-((1-(phenylsulfonyl)-1*H*-indol-4-yl)oxy)ethyl)amino)butyl)isoindoline-1,3-dione (**6**) (123 mg, 0.24 mmol), 40% aqueous solution of CH_3NH_2 (2.4 mL), 1 M $NaOH_{(aq)}$ (2.4 mL). The product was used without further purification. Yield: 78 mg (84%), yellowish oil. ^{1}H NMR (300 MHz, $CDCl_3$) δ 7.86 (d, J = 8.21 Hz, 2H), 7.60 (d, J = 8.21 Hz, 1H), 7.38–7.56 (m, 4H), 7.21 (t, J = 8.21 Hz, 1H), 6.78 (d, J = 3.52 Hz, 1H), 6.65 (d, J = 7.62 Hz, 1H), 4.16 (t, J = 4.98 Hz, 2H), 3.04 (t, J = 5.27 Hz, 2H), 2.70 (t, J = 6.74 Hz, 4H), 1.45–1.57 (m, 7H). Formula: $C_{20}H_{25}N_3O_3S$; MS: *m/z* 388 ($M + H^+$).

*4.1.10.3. N^1-(2-((1-(Phenylsulfonyl)-1H-indol-4-yl)oxy)ethyl)pentane-1,5-diamine (**12**).* Following **GP3**, compound **12** was prepared using 2-(5-((2-((1-(phenylsulfonyl)-1*H*-indol-4-yl)oxy)ethyl)amino)pentyl)isoindoline-1,3-dione (**7**) (159 mg, 0.30 mmol), 40% aqueous solution of CH_3NH_2 (3.0 mL), 1 M $NaOH_{(aq)}$ (3.0 mL). The product was used without further purification. Yield: 96 mg (80%), yellowish oil. ^{1}H NMR (300 MHz, $CDCl_3$) δ 7.83–7.90 (m, 2H), 7.59 (d, J = 8.21 Hz, 1H), 7.38–7.55 (m, 4H), 7.21 (t, J = 8.21 Hz, 1H), 6.77–6.80 (m, 1H), 6.65 (d, J = 7.62 Hz, 1H), 4.16 (t, J = 5.27 Hz, 2H), 3.03 (t, J = 5.27 Hz, 2H), 2.68 (t, J = 7.03 Hz, 4H), 1.78 (s, 3H), 1.31–1.58 (m, 6H). Formula: $C_{21}H_{27}N_3O_3S$; MS: *m/z* 402 ($M + H^+$).

4.1.11. General procedure for the synthesis of compounds 17–21 (GP4)

Step 1. A mixture of BOC-protected amine (**13**–**16**) or N^1-(2-((1-(phenylsulfonyl)-1H-indol-4-yl)oxy)ethyl)ethane-1,2-diamine (**9**) (1 equiv.), 9-chloro-1,2,3,4-tetrahydroacridine (1 equiv.) and pentan-1-ol was placed in a 5 mL microwave-transparent vial. The vial was capped and exposed to microwave heating at 190 °C for 120 min. After the mixture was cooled to room temperature, acetonitrile was removed, the residue was treated with saturated solution of $NaHCO_{3(aq)}$ and extracted with DCM. Combined organic fractions were washed with brine, dried over Na_2SO_4 and concentrated in vacuo. The crude product was purified by flash chromatography (DCM/MeOH/$NH_{3(aq)}$ 95:5:0.5). This yielded BOC-protected derivatives of compounds **19**–**21** and final products **17** and **18**. In case of compound **18** a spontaneous BOC-deprotection

took place during microwave-assisted reaction. Step 2. Next, BOC-protected derivatives of compounds **19**–**21** were dissolved in MeOH, 1 M HCl in EtOAc was added and the resulting mixture was stirred overnight at room temperature. After that time, the solution was concentrated on rotary evaporator, the residue was treated with saturated solution of $NaHCO_{3(aq)}$ and extracted with DCM. Combined organic fractions were washed with brine, dried over Na_2SO_4 and concentrated in vacuo. The crude product was purified by flash chromatography (DCM/MeOH/$NH_{3(aq)}$ 95:5:0.5).

*4.1.11.1. N^1-(2-((1-(phenylsulfonyl)-1H-indol-4-yl)oxy)ethyl)-N^2-(1,2,3,4-tetrahydroacridin-9-yl)ethane-1,2-diamine(**17**).*
Following **GP4**, compound **17** was prepared using N^1-(2-((1-(phenylsulfonyl)-1H-indol-4-yl)oxy)ethyl)ethane-1,2-diamine (**9**) (49 mg, 0.13 mmol), 9-chloro-1,2,3,4-tetrahydroacridine (28 mg, 0.13 mmol), pentan-1-ol (0.5 mL). Yield: 35 mg (50%), yellowish solid. Purity 97% (UPLC/MS). ^{1}H NMR (300 MHz, CD_3OD) δ 8.18 (d, J = 8.79 Hz, 1H), 7.82–7.88 (m, 2H), 7.68–7.73 (m, 1H), 7.49–7.64 (m, 3H), 7.31–7.47 (m, 4H), 7.17 (t, J = 8.21 Hz, 1H), 6.66 (dd, J = 1.76, 5.27 Hz, 2H), 4.11 (t, J = 4.98 Hz, 2H), 3.79 (t, J = 6.15 Hz, 2H), 2.96–3.08 (m, 4H), 2.79–2.88 (m, 2H), 2.53 (t, J = 6.15 Hz, 2H), 1.57–1.75 (m, 4H). ^{13}C NMR (75 MHz, CD_3OD) δ 153.9, 144.3, 143.1, 139.4, 137.6, 135.4 (2C), 131.8, 130.6, 128.0 (2C), 127.0, 126.1, 125.6, 125.5, 124.5, 122.6, 119.5, 115.3, 111.5, 107.8, 107.4, 105.9, 69.3, 54.9, 32.0, 31.0, 30.9, 25.3, 23.4, 22.8. Formula: $C_{31}H_{32}N_4O_3S$. HRMS: m/z found [M + H^+] 541.2215, $C_{31}H_{32}N_4O_3S$ requires 541.2273.

*4.1.11.2. N^1-(2-((1-(Phenylsulfonyl)-1H-indol-4-yl)oxy)ethyl)-N^3-(1,2,3,4-tetrahydroacridin-9-yl)propane-1,3-diamine (**18**).*
Following **GP4**, compound **18** was prepared using *tert*-butyl (3-aminopropyl)(2-((1-(phenylsulfonyl)-1H-indol-4-yl)oxy)ethyl) carbamate (**13**) (95 mg, 0.20 mmol), 9-chloro-1,2,3,4-tetrahydroacridine (43 mg, 0.20 mmol), pentan-1-ol (1 mL). Yield: 46 mg (41%), brownish solid. Purity 96% (UPLC/MS). ^{1}H NMR (300 MHz, $CDCl_3$) δ 8.03 (dd, J = 2.05, 8.50 Hz, 2H), 7.81–7.87 (m, 2H), 7.33–7.63 (m, 6H), 7.16–7.25 (m, 2H), 6.72 (d, J = 3.52 Hz, 1H), 6.63 (d, J = 7.62 Hz, 1H), 4.18 (t, J = 4.98 Hz, 2H), 3.82 (t, J = 6.15 Hz, 2H), 3.10 (t, J = 4.98 Hz, 2H), 2.92–3.03 (m, 4H), 2.52 (t, J = 6.45 Hz, 2H), 1.89 (quin, J = 5.86 Hz, 2H), 1.48–1.68 (m, 4H), NH signals not detected. ^{13}C NMR (75 MHz, $CDCl_3$) δ 155.0, 152.8, 152.1, 143.9, 138.0, 136.0, 133.8, 129.6, 129.2 (2C), 126.7 (2C), 125.6, 125.3, 124.7, 123.7, 123.6, 121.0, 118.1, 113.5, 106.7, 106.0, 104.3, 67.3, 49.3, 48.8, 31.4, 30.1, 30.0, 24.8, 22.3, 21.7. Formula: $C_{32}H_{34}N_4O_3S$. HRMS: m/z found [M + H^+] 555.2473, $C_{32}H_{34}N_4O_3S$ requires 555.2430.

*4.1.11.3. N^1-(2-((1-(Phenylsulfonyl)-1H-indol-4-yl)oxy)ethyl)-N^4-(1,2,3,4-tetrahydroacridin-9-yl)butane-1,4-diamine (**19**).*
Compound **19** was prepared following **GP4**. Step 1. *Tert*-butyl (4-aminobutyl)(2-((1-(phenylsulfonyl)-1H-indol-4-yl)oxy)ethyl) carbamate (**14**) (140 mg, 0.29 mmol), 9-chloro-1,2,3,4-tetrahydroacridine (63 mg, 0.29 mmol), pentan-1-ol (1.25 mL). Yield: 57 mg (29%), pale yellow solid. Formula: $C_{38}H_{44}N_4O_5S$; MS: m/z 669 (M + H^+). Step 2. Product from Step 1 (57 mg, 0.09 mmol), 1 M HCl in EtOAc (1 mL). Yield: 28 mg (55%). Purity 100% (UPLC/MS). ^{1}H NMR (300 MHz, $CDCl_3$) δ 7.92 (t, J = 9.67 Hz, 2H), 7.81–7.88 (m, 2H), 7.60 (d, J = 8.79 Hz, 1H), 7.47–7.56 (m, 2H), 7.45 (d, J = 3.52 Hz, 1H), 7.37–7.44 (m, 2H), 7.27–7.34 (m, 1H), 7.21 (t, J = 8.21 Hz, 1H), 6.75 (d, J = 3.52 Hz, 1H), 6.64 (d, J = 8.21 Hz, 1H), 4.14 (t, J = 5.27 Hz, 2H), 3.50 (t, J = 6.74 Hz, 2H), 2.98–3.08 (m, 4H), 2.64–2.76 (m, 4H), 1.81–1.94 (m, 4H), 1.55–1.79 (m, 4H), NH signals not detected. ^{13}C NMR (75 MHz, $CDCl_3$) δ 158.3, 152.3, 150.7, 147.3, 138.2, 136.2, 133.8, 129.2 (2C), 128.6, 128.3, 126.7 (2C), 125.7, 124.8, 123.6, 122.8, 121.2, 120.2, 115.9, 106.7, 106.2, 104.5, 67.6, 49.3, 48.7, 33.9, 31.5, 29.4, 27.6, 24.8, 23.0, 22.7. Formula: $C_{33}H_{36}N_4O_3S$. HRMS: m/z found [M + H^+] 569.2527, $C_{33}H_{36}N_4O_3S$ requires 569.2586.

*4.1.11.4. N^1-(2-((1-(Phenylsulfonyl)-1H-indol-4-yl)oxy)ethyl)-N^5-(1,2,3,4-tetrahydroacridin-9-yl)pentane-1,5-diamine (**20**).*
Compound **20** was prepared following **GP4**. Step 1. *Tert*-butyl (5-aminopentyl)(2-((1-(phenylsulfonyl)-1H-indol-4-yl)oxy)ethyl) carbamate (**15**) (40 mg, 0.08 mmol), 9-chloro-1,2,3,4-tetrahydroacridine (17 mg, 0.08 mmol), pentan-1-ol (0.5 mL). Yield: 18 mg (33%). Formula: $C_{39}H_{46}N_4O_5S$; MS: m/z 683 (M + H^+). Step 2. Product from Step 1 (18 mg, 0.026 mmol), 1 M HCl in EtOAc (1 mL). Yield: 8 mg (53%), brownish oil. Purity 98% (UPLC/MS). ^{1}H NMR (300 MHz, $CDCl_3$) δ 7.88–7.96 (m, 2H), 7.82–7.87 (m, 2H), 7.59 (d, J = 8.21 Hz, 1H), 7.46–7.57 (m, 2H), 7.36–7.46 (m, 3H), 7.32 (ddd, J = 1.17, 6.89, 8.35 Hz, 1H), 7.20 (t, J = 8.21 Hz, 1H), 6.73–6.78 (m, 1H), 6.64 (d, J = 8.21 Hz, 1H), 4.14 (t, J = 5.27 Hz, 2H), 3.47 (t, J = 7.33 Hz, 2H), 2.98–3.08 (m, 4H), 2.67 (t, J = 7.03 Hz, 4H), 1.83–1.95 (m, 4H), 1.67 (quin, J = 7.33 Hz, 2H), 1.39–1.59 (m, 4H), NH signals not detected. Formula: $C_{34}H_{38}N_4O_3S$. HRMS: m/z found [M + H^+] 583.2746, $C_{34}H_{38}N_4O_3S$ requires 583.2743.

*4.1.11.5. N^1-(2-((1-(Phenylsulfonyl)-1H-indol-4-yl)oxy)ethyl)-N^6-(1,2,3,4-tetrahydroacridin-9-yl)hexane-1,6-diamine (**21**).*
Compound **21** was prepared following **GP4**. Step 1. *Tert*-butyl (6-aminohexyl)(2-((1-(phenylsulfonyl)-1H-indol-4-yl)oxy)ethyl) carbamate (**16**) (73 mg, 0.14 mmol), 9-chloro-1,2,3,4-tetrahydroacridine (30 mg, 0.14 mmol), pentan-1-ol (0.5 mL). Yield: 49 mg (50%). Formula: $C_{40}H_{48}N_4O_5S$; MS: m/z 670 (M + H^+). Step 2. Product from Step 1 (49 mg, 0.07 mmol), 1 M HCl in EtOAc (1.5 mL). Yield: 25 mg (60%), pale yellow solid. Purity 99% (UPLC/MS). ^{1}H NMR (300 MHz, $CDCl_3$) δ 7.89–7.97 (m, 2H), 7.82–7.88 (m, 2H), 7.59 (d, J = 8.21 Hz, 1H), 7.47–7.57 (m, 2H), 7.37–7.47 (m, 3H), 7.33 (ddd, J = 1.17, 6.89, 8.35 Hz, 1H), 7.20 (t, J = 8.21 Hz, 1H), 6.76 (d, J = 3.52 Hz, 1H), 6.64 (d, J = 8.21 Hz, 1H), 4.15 (t, J = 5.28 Hz, 2H), 3.47 (t, J = 7.33 Hz, 2H), 2.98–3.10 (m, 4H), 2.62–2.73 (m, 4H), 1.85–1.96 (m, 4H), 1.66 (quin, J = 7.18 Hz, 2H), 1.45–1.56 (m, 2H), 1.34–1.43 (m, 4H), NH signals not detected. ^{13}C NMR (75 MHz, $CDCl_3$) δ 158.3, 152.3, 150.8, 147.2, 138.2, 136.2, 133.8, 129.2 (2C), 128.6, 128.4, 126.7 (2C), 125.7, 124.8, 123.6, 122.8, 121.2, 120.1, 115.8, 106.6, 106.2, 104.6, 67.7, 49.7, 49.4, 48.7, 33.9, 31.7, 30.0, 27.0, 26.9, 24.8, 23.0, 22.7. Formula: $C_{35}H_{40}N_4O_3S$. HRMS: m/z found [M + H^+] 597.3077, $C_{35}H_{40}N_4O_3S$ requires 597.2899.

4.1.12. General procedure for the synthesis of compounds 22–35 (GP5)

To an adequate amine (1.3 equiv.) dissolved in MeOH, aldehyde (1 equiv.) and glacial acetic acid (catalytic amounts) were added. After 1 h of stirring at ambient temperature, the reaction mixture was cooled on an ice bath and $NaBH_3CN$ (3 equiv.) was added. The reaction was stirred 18 h at room temperature. Then, the solvents were removed in vacuo, the residue was treated with water and extracted with DCM. Combined organic fractions were washed with brine, dried over Na_2SO_4 and concentrated in vacuo. The crude product was purified by methods described below.

*4.1.12.1. N^1-Benzyl-N^2-(2-((1-(phenylsulfonyl)-1H-indol-4-yl)oxy)ethyl)ethane-1,2-diamine (**22**).* Following GP5, compound **22** was prepared using N^1-(2-((1-(phenylsulfonyl)-1H-indol-4-yl)oxy)ethyl)ethane-1,2-diamine (**9**) (66 mg, 0.18 mmol), benzaldehyde (14 μL, 0.14 mmol), glacial acetic acid (20 μL), $NaBH_3CN$ (26 mg, 0.42 mmol) in 3 mL MeOH. Purification: column chromatography (DCM/MeOH/$NH_{3(aq)}$ 90:10:0.5). Yield: 45 mg (71%), colourless oil. Purity 100% (UPLC/MS). ^{1}H NMR (300 MHz, $CDCl_3$) δ 7.83–7.90 (m, 2H), 7.60 (d, J = 8.21 Hz, 1H), 7.48–7.55 (m, 1H), 7.37–7.47 (m, 3H), 7.17–7.33 (m, 6H), 6.78 (d, J = 3.52 Hz, 1H), 6.65 (d, J = 8.21 Hz, 1H), 4.15 (t, J = 5.27 Hz, 2H), 3.79 (s, 2H), 3.03 (t, J = 5.27 Hz, 2H),

2.73–2.85 (m, 4H), 1.87 (br. s., 2H). ^{13}C NMR (75 MHz, CHLOROFORM-d) δ 152.3, 140.3, 138.2, 136.1, 133.7, 129.2 (2C), 128.3 (2C), 128.0, 126.9, 126.7 (2C), 125.6 (2C), 124.7, 121.2, 106.6, 106.3, 104.5, 67.7, 53.8, 49.1, 48.7, 48.5. Formula: $C_{25}H_{27}N_3O_3S$. HRMS: *m/z* found [M + H$^+$] 450.1939, $C_{25}H_{27}N_3O_3S$ requires 450.1851.

*4.1.12.2. N^1-Benzyl-N^3-(2-((1-(phenylsulfonyl)-1H-indol-4-yl)oxy) ethyl)propane-1,3-diamine (**23**).* Following GP5, compound **23** was prepared using N^1-(2-((1-(phenylsulfonyl)-1H-indol-4-yl)oxy) ethyl)propane-1,3-diamine (**10**) (77 mg, 0.21 mmol), benzaldehyde (16 μL, 0.16 mmol), glacial acetic acid (20 μL), $NaBH_3CN$ (30 mg, 0.48 mmol) in 3 mL MeOH. Purification: column chromatography (DCM/MeOH/$NH_{3(aq)}$ 95:5:0.5). Yield: 38 mg (51%), yellowish oil. Purity 95% (UPLC/MS). ^{1}H NMR (300 MHz, $CDCl_3$) δ 7.83–7.89 (m, 2H), 7.60 (d, *J* = 8.21 Hz, 1H), 7.48–7.54 (m, 1H), 7.46 (d, *J* = 4.10 Hz, 1H), 7.37–7.44 (m, 2H), 7.25–7.31 (m, 4H), 7.17–7.25 (m, 2H), 6.74–6.78 (m, 1H), 6.65 (d, *J* = 7.62 Hz, 1H), 4.15 (t, *J* = 5.28 Hz, 2H), 3.77 (s, 2H), 3.03 (t, *J* = 5.27 Hz, 2H), 2.77 (t, *J* = 7.03 Hz, 2H), 2.72 (t, *J* = 6.74 Hz, 2H), 1.87 (br. s., 2H), 1.73 (t, *J* = 7.03 Hz, 2H). ^{13}C NMR (75 MHz, $CDCl_3$) δ ppm 152.3, 140.0, 138.2, 136.1, 133.7, 129.2 (2C), 128.3 (2C), 128.0, 126.8, 126.7 (2C), 125.6 (2C), 124.7, 121.2, 106.6, 106.3, 104.6, 67.6, 53.9, 48.7, 48.4, 47.8, 29.9. Formula: $C_{26}H_{29}N_3O_3S$. HRMS: *m/z* found [M + H$^+$] 464.1979, $C_{26}H_{29}N_3O_3S$ requires 464.2008.

*4.1.12.3. N^1-Benzyl-N^4-(2-((1-(phenylsulfonyl)-1H-indol-4-yl)oxy) ethyl)butane-1,4-diamine (**24**).* Following GP5, compound **24** was prepared using N^1-(2-((1-(phenylsulfonyl)-1H-indol-4-yl)oxy) ethyl)butane-1,4-diamine (**11**) (78 mg, 0.20 mmol), benzaldehyde (15 μL, 0.15 mmol), glacial acetic acid (20 μL), $NaBH_3CN$ (28 mg, 0.45 mmol) in 3 mL MeOH. Purification: column chromatography (DCM/MeOH/$NH_{3(aq)}$ 95:5:0.5). Yield: 31 mg (43%), yellowish oil. Purity 96% (UPLC/MS). ^{1}H NMR (300 MHz, $CDCl_3$) δ 7.83–7.88 (m, 2H), 7.60 (d, *J* = 8.21 Hz, 1H), 7.48–7.55 (m, 1H), 7.47 (d, *J* = 3.52 Hz, 1H), 7.37–7.45 (m, 2H), 7.29–7.33 (m, 3H), 7.17–7.29 (m, 3H), 6.77 (d, *J* = 3.52 Hz, 1H), 6.64 (d, *J* = 7.62 Hz, 1H), 4.14 (t, *J* = 5.28 Hz, 2H), 3.77 (s, 2H), 3.03 (t, *J* = 5.27 Hz, 2H), 2.61–2.73 (m, 4H), 1.68 (br. s., 2H), 1.52–1.60 (m, 4H). ^{13}C NMR (75 MHz, CHLOROFORM-d) δ. ^{13}C NMR (75 MHz, $CDCl_3$) δ 152.3, 138.2, 136.1, 133.7, 129.2 (2C), 128.7, 128.3 (2C), 128.1, 126.9, 126.7 (2C), 125.6 (2C), 124.7, 121.2, 106.6, 106.2, 104.5, 67.6, 53.9, 49.6, 49.1, 48.6, 27.9, 27.8. Formula: $C_{27}H_{31}N_3O_3S$. HRMS: *m/z* found [M + H$^+$] 478.2169, $C_{27}H_{31}N_3O_3S$ requires 478.2164.

*4.1.12.4. N^1-Benzyl-N^5-(2-((1-(phenylsulfonyl)-1H-indol-4-yl)oxy) ethyl)pentane-1,5-diamine (**25**).* Following GP5, compound **25** was prepared using N^1-(2-((1-(phenylsulfonyl)-1H-indol-4-yl)oxy) ethyl)pentane-1,5-diamine (**12**) (96 mg, 0.24 mmol), benzaldehyde (18 μL, 0.18 mmol), glacial acetic acid (20 μL), $NaBH_3CN$ (34 mg, 0.54 mmol) in 3 mL MeOH. Purification: column chromatography (DCM/MeOH/$NH_{3(aq)}$ 97:3:0.25). Yield: 20 mg (23%), colourless oil. Purity 100% (UPLC/MS). ^{1}H NMR (300 MHz, $CDCl_3$) δ 7.83–7.89 (m, 2H), 7.60 (d, *J* = 8.21 Hz, 1H), 7.48–7.55 (m, 1H), 7.38–7.48 (m, 3H), 7.28–7.34 (m, 4H), 7.18–7.25 (m, 2H), 6.78 (d, *J* = 3.52 Hz, 1H), 6.65 (d, *J* = 7.62 Hz, 1H), 4.15 (t, *J* = 5.27 Hz, 2H), 3.76–3.80 (m, 2H), 3.03 (t, *J* = 5.27 Hz, 2H), 2.59–2.72 (m, 4H), 1.64 (br. s., 2H), 1.48–1.57 (m, 4H), 1.36–1.43 (m, 2H). ^{13}C NMR (75 MHz, $CDCl_3$) δ 152.3, 140.3, 138.2, 136.2, 133.7, 129.2 (2C), 128.4 (2C), 128.1, 126.9, 126.7 (2C), 125.7 (2C), 124.7, 121.2, 106.6, 106.3, 104.6, 67.7, 54.0, 49.7, 49.3, 48.7, 30.0, 29.7, 25.0. Formula: $C_{28}H_{33}N_3O_3S$. HRMS: *m/z* found [M + H$^+$] 492.2363, $C_{28}H_{33}N_3O_3S$ requires 492.2321.

*4.1.12.5. N^1-(2-Chlorobenzyl)-N^2-(2-((1-(phenylsulfonyl)-1H-indol-4-yl)oxy)ethyl)ethane-1,2-diamine (**26**).* Following GP5, compound **26** was prepared using N^1-(2-((1-(phenylsulfonyl)-1H-indol-4-yl) oxy)ethyl)ethane-1,2-diamine (**9**) (65 mg, 0.18 mmol), 2-chlorobenzaldehyde (16 μL, 0.14 mmol), glacial acetic acid (20 μL), $NaBH_3CN$ (26 mg, 0.42 mmol) in 3 mL MeOH. Purification: flash chromatography (DCM/1% NH_3 in MeOH 93:7). Yield: 54 mg (80%), colourless oil. Purity 97% (UPLC/MS). ^{1}H NMR (300 MHz, $CDCl_3$) δ 7.83–7.89 (m, 2H), 7.60 (d, *J* = 8.21 Hz, 1H), 7.47–7.55 (m, 1H), 7.29–7.47 (m, 5H), 7.14–7.24 (m, 3H), 6.76 (d, *J* = 2.93 Hz, 1H), 6.64 (d, *J* = 7.62 Hz, 1H), 4.16 (t, *J* = 5.27 Hz, 2H), 3.88 (s, 2H), 3.05 (t, *J* = 5.27 Hz, 2H), 2.75–2.88 (m, 4H), 2.29 (br. s., 2H). ^{13}C NMR (75 MHz, $CDCl_3$) δ 152.2, 138.1, 137.3, 136.1, 133.7, 133.7, 130.1, 129.4, 129.2 (2C), 128.3, 126.8, 126.7 (2C), 125.6, 124.7, 121.2, 106.6, 106.3, 104.5, 67.4, 51.1, 48.8, 48.4, 48.2. Formula: $C_{25}H_{26}ClN_3O_3S$. HRMS: *m/z* found [M + H$^+$] 484.1406, $C_{25}H_{26}ClN_3O_3S$ requires 484.1461.

*4.1.12.6. N^1-(3-Chlorobenzyl)-N^2-(2-((1-(phenylsulfonyl)-1H-indol-4-yl)oxy)ethyl)ethane-1,2-diamine (**27**).* Following GP5, compound **27** was prepared using N^1-(2-((1-(phenylsulfonyl)-1H-indol-4-yl) oxy)ethyl)ethane-1,2-diamine (**9**) (63 mg, 0.18 mmol), 3-chlorobenzaldehyde (16 μL, 0.14 mmol), glacial acetic acid (20 μL), $NaBH_3CN$ (26 mg, 0.42 mmol) in 3 mL MeOH. Purification: flash chromatography (DCM/10% NH_3 in MeOH 90:10). Yield: 57 mg (84%), colourless oil. Purity 98% (UPLC/MS). ^{1}H NMR (300 MHz, $CDCl_3$) δ 7.82–7.89 (m, 2H), 7.60 (d, *J* = 8.21 Hz, 1H), 7.48–7.55 (m, 1H), 7.37–7.47 (m, 3H), 7.31 (s, 1H), 7.15–7.24 (m, 4H), 6.77 (d, *J* = 3.52 Hz, 1H), 6.64 (d, *J* = 7.62 Hz, 1H), 4.16 (t, *J* = 5.27 Hz, 2H), 3.76 (s, 2H), 3.04 (t, *J* = 4.98 Hz, 2H), 2.80–2.86 (m, 2H), 2.71–2.79 (m, 2H), 2.15 (br. s., 2H). ^{13}C NMR (75 MHz, $CDCl_3$) δ 152.2, 142.2, 138.2, 136.1, 134.2, 133.8, 129.6, 129.2 (2C), 128.1, 127.1, 126.7 (2C), 126.2, 125.6, 124.8, 121.2, 106.7, 106.3, 104.5, 67.4, 53.2, 48.8, 48.4, 48.3. Formula: $C_{25}H_{26}ClN_3O_3S$. HRMS: *m/z* found [M + H$^+$] 484.1556, $C_{25}H_{26}ClN_3O_3S$ requires 484.1461.

*4.1.12.7. N^1-(4-Chlorobenzyl)-N^2-(2-((1-(phenylsulfonyl)-1H-indol-4-yl)oxy)ethyl)ethane-1,2-diamine (**28**).* Following GP5, compound **28** was prepared using N^1-(2-((1-(phenylsulfonyl)-1H-indol-4-yl) oxy)ethyl)ethane-1,2-diamine (**9**) (66 mg, 0.18 mmol), 4-chlorobenzaldehyde (20 mg, 0.14 mmol), glacial acetic acid (20 μL), $NaBH_3CN$ (26 mg, 0.42 mmol) in 3 mL MeOH. Purification: flash chromatography (DCM/1% NH_3 in MeOH 90:10). Yield: 61 mg (90%), colourless oil. Purity 95% (UPLC/MS). ^{1}H NMR (300 MHz, $CDCl_3$) δ 7.87–7.93 (m, 2H) 7.64 (d, *J* = 8.2 Hz, 1H) 7.51–7.59 (m, 1H) 7.41–7.51 (m, 3H) 7.21–7.28 (m, 4H) 6.79 (d, *J* = 2.9 Hz, 1H) 6.67 (d, *J* = 7.6 Hz, 1H) 4.18 (t, *J* = 5.3 Hz, 2H) 3.79 (s, 2H) 3.07 (t, *J* = 5.3 Hz, 2H) 2.82–2.89 (m, 2H) 2.75–2.81 (m, 2H) 2.25 (s, 3H). ^{13}C NMR (75 MHz, $CDCl_3$) δ 152.2, 138.3, 136.1, 133.8, 132.7, 129.5 (2C), 129.2 (2C), 128.5 (2C), 126.7 (2C), 125.6, 124.7, 121.2, 110.0, 106.7, 106.2, 104.5, 67.4, 52.9, 48.7, 48.4, 48.2. Formula: $C_{25}H_{26}ClN_3O_3S$. HRMS: *m/z* found [M + H$^+$] 484.1504, $C_{25}H_{26}ClN_3O_3S$ requires 484.1461.

*4.1.12.8. N^1-(3,5-Dichlorobenzyl)-N^2-(2-((1-(phenylsulfonyl)-1H-indol-4-yl)oxy)ethyl)ethane-1,2-diamine (**29**).* Following GP5, compound **29** was prepared using N^1-(2-((1-(phenylsulfonyl)-1H-indol-4-yl)oxy)ethyl)ethane-1,2-diamine (**9**) (63 mg, 0.18 mmol), 3,5-dichlorobenzaldehyde (25 mg, 0.14 mmol), glacial acetic acid (20 μL), $NaBH_3CN$ (26 mg, 0.42 mmol) in 3 mL MeOH. Purification: flash chromatography (DCM/1% NH_3 in MeOH 90:10). Yield: 64 mg (88%), colourless oil. Purity 98% (UPLC/MS). ^{1}H NMR (300 MHz, $CDCl_3$) δ 7.82–7.90 (m, 2H), 7.60 (d, *J* = 8.79 Hz, 1H), 7.37–7.55 (m, 4H), 7.13–7.25 (m, 4H), 6.77 (d, *J* = 3.52 Hz, 1H), 6.64 (d, *J* = 7.62 Hz, 1H), 4.17 (t, *J* = 4.98 Hz, 2H), 3.73 (s, 2H), 3.05 (t, *J* = 4.98 Hz, 2H),

2.78–2.87 (m, 2H), 2.70–2.77 (m, 2H), 2.30 (br. s., 2H). ^{13}C NMR (75 MHz, $CDCl_3$) δ 143.9, 138.2, 136.1, 134.8, 133.8 (2C), 129.2 (2C), 127.1, 126.7 (2C), 126.4 (2C), 125.6, 124.8, 121.2, 106.8, 106.7, 106.2, 104.5, 67.4, 52.8, 48.8, 48.4, 48.4. Formula: $C_{25}H_{25}Cl_2N_3O_3S$. HRMS: *m/z* found [M + H$^+$] 518.1061, $C_{25}H_{25}Cl_2N_3O_3S$ requires 518.1072.

*4.1.12.9. N^1-(4-Fluorobenzyl)-N^2-(2-((1-(phenylsulfonyl)-1H-indol-4-yl)oxy)ethyl)ethane-1,2-diamine (**30**).* Following GP5, compound **30** was prepared using N^1-(2-((1-(phenylsulfonyl)-1H-indol-4-yl) oxy)ethyl)ethane-1,2-diamine (**9**) (65 mg, 0.18 mmol), 4-fluorobenzaldehyde (15 μL, 0.14 mmol), glacial acetic acid (20 μL), $NaBH_3CN$ (26 mg, 0.42 mmol) in 3 mL MeOH. Purification: flash chromatography (DCM/1% NH_3 in MeOH 90:10). Yield: 56 mg (86%), colourless oil. Purity 97% (UPLC/MS). ^{1}H NMR (300 MHz, CD_3OD) δ 7.85–7.93 (m, 2H), 7.42–7.61 (m, 5H), 7.27–7.36 (m, 2H), 7.22 (t, *J* = 8.21 Hz, 1H), 6.94–7.05 (m, 2H), 6.84 (d, *J* = 3.52 Hz, 1H), 6.73 (d, *J* = 7.62 Hz, 1H), 4.17 (t, *J* = 5.27 Hz, 2H), 3.71–3.77 (m, 2H), 3.04 (t, *J* = 4.98 Hz, 2H), 2.80–2.87 (m, 2H), 2.72–2.79 (m, 2H), –NH– signals non-detectable due to H–D exchange. ^{13}C NMR (75 MHz, CD_3OD) δ ppm 162.1 (d, *J* = 244.20 Hz), 152.2, 137.8, 136.1, 134.7 (d, *J* = 2.30 Hz), 133.8, 130.1 (d, *J* = 8.06 Hz, 2C), 129.0 (2C), 126.5 (2C), 125.4, 124.7, 121.2, 114.8, 114.6, 106.3 (d, *J* = 18.43 Hz, 2C), 104.4, 66.6, 51.9, 48.4, 48.2, 47.9. Formula: $C_{25}H_{26}FN_3O_3S$. HRMS: *m/z* found [M + H$^+$] 468.1809, $C_{25}H_{26}FN_3O_3S$ requires 468.1757.

*4.1.12.10. N^1-(4-Nitrobenzyl)-N^2-(2-((1-(phenylsulfonyl)-1H-indol-4-yl)oxy)ethyl)ethane-1,2-diamine (**31**).* Following GP5, compound **31** was prepared using N^1-(2-((1-(phenylsulfonyl)-1H-indol-4-yl) oxy)ethyl)ethane-1,2-diamine (**9**) (65 mg, 0.18 mmol), 4-nitrobenzaldehyde (21 mg, 0.14 mmol), glacial acetic acid (20 μL), $NaBH_3CN$ (26 mg, 0.42 mmol) in 3 mL MeOH. Purification: flash chromatography (DCM/1% NH_3 in MeOH 93:7). Yield: 50 mg (72%), dark orange oil. Purity 100% (UPLC/MS). ^{1}H NMR (300 MHz, $CDCl_3$) δ 8.08–8.16 (m, 2H), 7.84–7.90 (m, 2H), 7.61 (d, *J* = 8.21 Hz, 1H), 7.38–7.56 (m, 6H), 7.22 (t, *J* = 8.21 Hz, 1H), 6.76 (d, *J* = 4.69 Hz, 1H), 6.65 (d, *J* = 7.62 Hz, 1H), 4.16 (t, *J* = 4.98 Hz, 2H), 3.88 (s, 2H), 3.05 (t, *J* = 4.98 Hz, 2H), 2.80–2.87 (m, 2H), 2.71–2.79 (m, 2H), 1.95 (br. s., 2H). ^{13}C NMR (75 MHz, $CDCl_3$) δ 152.2, 148.1, 146.9, 138.1, 136.1, 133.8, 129.2 (2C), 128.5 (2C), 126.7 (2C), 125.6, 124.7, 123.5 (2C), 121.1, 106.6, 106.1, 104.5, 67.5, 53.0, 48.9, 48.7, 48.5. Formula: $C_{25}H_{26}N_4O_5S$. HRMS: *m/z* found [M + H$^+$] 495.2026, $C_{25}H_{26}N_4O_5S$ requires 495.1702.

*4.1.12.11. N^1-(4-Methoxybenzyl)-N^2-(2-((1-(phenylsulfonyl)-1H-indol-4-yl)oxy)ethyl)ethane-1,2-diamine (**32**).* Following GP5, compound **32** was prepared using N^1-(2-((1-(phenylsulfonyl)-1H-indol-4-yl)oxy)ethyl)ethane-1,2-diamine (**9**) (65 mg, 0.18 mmol), 4-methoxybenzaldehyde (17 μL, 0.14 mmol), glacial acetic acid (20 μL), $NaBH_3CN$ (26 mg, 0.42 mmol) in 3 mL MeOH. Purification: flash chromatography (DCM/1% NH_3 in MeOH 90:10). Yield: 43 mg (64%), yellowish oil. Purity 100% (UPLC/MS). ^{1}H NMR (300 MHz, $CDCl_3$) δ 7.82–7.88 (m, 2H), 7.59 (d, *J* = 8.21 Hz, 1H), 7.47–7.55 (m, 1H), 7.37–7.46 (m, 3H), 7.15–7.28 (m, 3H), 6.75–6.85 (m, 3H), 6.62 (d, *J* = 8.21 Hz, 1H), 4.13 (t, *J* = 5.27 Hz, 2H), 3.78 (s, 2H), 3.76 (s, 3H), 3.19 (br. s., 2H), 3.01 (t, *J* = 4.98 Hz, 2H), 2.83–2.89 (m, 2H), 2.75–2.82 (m, 2H). ^{13}C NMR (75 MHz, $CDCl_3$) δ 159.0, 152.1, 138.1, 136.1, 133.8, 129.8 (2C), 129.6, 129.2 (2C), 126.7 (2C), 125.6, 124.8, 121.1, 113.9 (2C), 106.7, 106.3, 104.5, 67.3, 55.2, 52.4, 48.2, 47.7, 47.3. Formula: $C_{26}H_{29}N_3O_4S$. HRMS: *m/z* found [M + H$^+$] 480.1933, $C_{26}H_{29}N_3O_4S$ requires 480.1957.

*4.1.12.12. N^1-(3-Methylbenzyl)-N^2-(2-((1-(phenylsulfonyl)-1H-indol-4-yl)oxy)ethyl)ethane-1,2-diamine (**33**).* Following GP5, compound **33** was prepared using N^1-(2-((1-(phenylsulfonyl)-1H-indol-4-yl) oxy)ethyl)ethane-1,2-diamine (**9**) (86 mg, 0.24 mmol), 3-methylbenzaldehyde (21 μL, 0.18 mmol), glacial acetic acid (20 μL), $NaBH_3CN$ (34 mg, 0.54 mmol) in 4 mL MeOH. Purification: flash chromatography (DCM/1% NH_3 in MeOH 90:10). Yield: 43 mg (41%), colourless oil. Purity 100% (UPLC/MS). ^{1}H NMR (300 MHz, $CDCl_3$) δ 7.82–7.88 (m, 2H), 7.59 (d, *J* = 8.21 Hz, 1H), 7.46–7.54 (m, 1H), 7.36–7.46 (m, 3H), 7.09–7.24 (m, 4H), 7.05 (d, *J* = 7.03 Hz, 1H), 6.75–6.81 (m, 1H), 6.62 (d, *J* = 7.62 Hz, 1H), 4.14 (t, *J* = 5.28 Hz, 2H), 3.81 (s, 2H), 3.38 (br. s., 2H), 3.02 (t, *J* = 5.27 Hz, 2H), 2.84–2.91 (m, 2H), 2.76–2.84 (m, 2H), 2.29 (s, 3H). ^{13}C NMR (75 MHz, $CDCl_3$) δ 152.1, 138.2, 138.1, 137.5, 136.1, 133.7, 129.3, 129.2 (2C), 128.4, 128.3, 126.6 (2C), 125.6, 125.5, 124.8, 121.1, 106.7, 106.3, 104.5, 67.1, 52.9, 48.1, 47.6, 47.2, 21.3. Formula: $C_{26}H_{29}N_3O_3S$. HRMS: *m/z* found [M + H$^+$] 464.2049, $C_{26}H_{29}N_3O_3S$ requires 464.2008.

*4.1.12.13. N^1-(3-Trifluoromethylbenzyl)-N^2-(2-((1-(phenylsulfonyl)-1H-indol-4-yl)oxy)ethyl)ethane-1,2-diamine (**34**).* Following GP5, compound **34** was prepared using N^1-(2-((1-(phenylsulfonyl)-1H-indol-4-yl)oxy)ethyl)ethane-1,2-diamine (**9**) (64 mg, 0.18 mmol), 3-trifluoromethylbenzaldehyde (19 μL, 0.14 mmol), glacial acetic acid (20 μL), $NaBH_3CN$ (26 mg, 0.42 mmol) in 3 mL MeOH. Purification: flash chromatography (DCM/1% NH_3 in MeOH 90:10). Yield: 46 mg (63%), dark orange oil. Purity 100% (UPLC/MS). ^{1}H NMR (300 MHz, $CDCl_3$) δ 7.83–7.89 (m, 2H), 7.35–7.63 (m, 9H), 7.21 (t, *J* = 8.21 Hz, 1H), 6.74–6.78 (m, 1H), 6.64 (d, *J* = 7.62 Hz, 1H), 4.16 (t, *J* = 5.27 Hz, 2H), 3.84 (s, 2H), 3.04 (t, *J* = 4.98 Hz, 2H), 2.81–2.87 (m, 2H), 2.73–2.80 (m, 2H), 2.02 (br. s., 2H). ^{13}C NMR (126 MHz, $CDCl_3$) δ 151.8, 139.8, 138.1, 136.1, 133.8, 131.7, 130.7 (d, *J* = 32.0 Hz), 129.2 (2C), 129.0, 126.7 (2C), 125.6, 124.9 (br d, *J* = 3.6 Hz), 124.9, 124.2 (br d, *J* = 4.2 Hz), 121.1, 124.0 (q, *J* = 272.2 Hz), 107.0, 106.3, 104.5, 66.1, 52.7, 47.7, 47.6, 46.7. Formula: $C_{26}H_{26}F_3N_3O_3S$. HRMS: *m/z* found [M + H$^+$] 518.1878, $C_{26}H_{26}F_3N_3O_3S$ requires 518.1725.

*4.1.12.14. 3-(((2-((2-((1-(Phenylsulfonyl)-1H-indol-4-yl)oxy)ethyl) amino)ethyl)amino)methyl)phenyl ethyl(methyl)carbamate (**35**).* Following GP5, compound **35** was prepared using N^1-(2-((1-(phenylsulfonyl)-1H-indol-4-yl)oxy)ethyl)ethane-1,2-diamine (**9**) (64 mg, 0.18 mmol), 3-formylphenyl ethyl(methyl)carbamate (29 mg, 0.14 mmol), glacial acetic acid (20 μL), $NaBH_3CN$ (26 mg, 0.42 mmol) in 3 mL MeOH. Purification: flash chromatography (DCM/1% NH_3 in MeOH 90:10). Yield: 41 mg (53%), colourless oil. Purity 100% (UPLC/MS). ^{1}H NMR (300 MHz, $CDCl_3$) δ 7.82–7.89 (m, 2H), 7.59 (d, *J* = 8.79 Hz, 1H), 7.47–7.55 (m, 1H), 7.37–7.47 (m, 3H), 7.08–7.30 (m, 4H), 6.98 (d, *J* = 7.62 Hz, 1H), 6.79 (d, *J* = 3.52 Hz, 1H), 6.63 (d, *J* = 8.21 Hz, 1H), 4.16 (t, *J* = 5.27 Hz, 2H), 3.80 (s, 2H), 3.30–3.46 (m, 2H), 3.04 (t, *J* = 4.98 Hz, 2H), 2.97 (d, *J* = 18.76 Hz, 3H), 2.75–2.87 (m, 4H), 2.55 (br. s., 2H), 1.17 (t, *J* = 13.48 Hz, 3H). ^{13}C NMR (75 MHz, $CDCl_3$) δ 152.1, 151.6, 140.8, 138.1, 133.8, 129.3, 129.2 (2C), 129.2, 126.7 (2C), 125.6, 125.0, 124.8, 121.6, 121.2, 120.7, 120.6, 106.7, 106.3, 104.5, 67.0, 53.1, 48.3, 48.1, 47.7, 44.0, 13.2, 12.4. Formula: $C_{29}H_{34}N_4O_5S$. HRMS: *m/z* found [M + H$^+$] 551.2234, $C_{29}H_{34}N_4O_5S$ requires 551.2328.

4.2. Molecular docking studies

Prediction of protein-ligand interactions was based on molecular docking to the previously developed homology models of the 5-HT_6 receptors and experimental structures of BuChE. Procedure for obtaining ligand-optimized models of high predictive value, utilizing induced fit docking (IFD), was characterized in detail previously [66,83]. The 5-HT_6 receptor model was based on the 5-HT_{1B} serotonin receptor crystal structure (PDB ID: 4IAR) [84] and

the BuChE receptor was based on the previously determined X-ray structure in complex with a similar family ligand (PDB ID: 7AWG). Ligand structures were optimized using LigPrep tool and docked by Glide SP flexible docking procedure using OPLS3 force field. H-bond constraint, as well as centroid of a grid box were located on Asp3.32[106] residue for 5-HTR and on the bound ligand in human BuChE. Selection of the binding mode was based on scoring function and manual interaction analysis. The docking procedure was followed by system relaxation into a local energy minimum using a hybrid method of the steepest decent and the LM-BFGS algorithms. Small-Molecule Drug Discovery Suite (Schrödinger, Inc.) was licensed for Jagiellonian University Medical College.

4.3. 5-HT_6 receptor binding assay

Preparation of solutions of test and reference compounds. 10 mM stock solutions of tested compounds were prepared in DMSO. Serial dilutions of compounds were prepared in 96-well microplate in assay buffers using automated pipetting system epMotion 5070 (Eppendorf). Each compound was tested in 8 concentrations from 10−5 to 10−12 M (final concentration). **Radioligand binding** was performed using membranes from CHO−K1 cells stably transfected with the human 5-HT_6 receptor (PerkinElmer). All assays were carried out in duplicates. 50 μl working solution of the tested compounds, 50 μl [^{3}H]-LSD (final concentration 2.5 nM) and 150 μl diluted membranes (15 μg protein per well) prepared in assay buffer (50 mM Tris, pH 7.4, 10 mM $MgCl_2$, 0.1 mM EDTA) were transferred to polypropylene 96-well microplate using 96-wells pipetting station Rainin Liquidator (MettlerToledo). Methiothepin (10 μM) was used to define nonspecific binding. Microplate was covered with a sealing tape, mixed and incubated for 60 min at 27 °C. The reaction was terminated by rapid filtration through GF/B filter mate presoaked with 0.5% polyethyleneimine for 30 min. Ten rapid washes with 200 μl 50 mM Tris buffer (4 °C, pH 7.4) were performed using automated harvester system Harvester-96 MACH III FM (Tomtec). The filter mates were dried at 37 °C in forced air fan incubator and then solid scintillator MeltiLex was melted on filter mates at 90 °C for 5 min. Radioactivity was counted in MicroBeta2 scintillation counter (PerkinElmer). Data were fitted to a one-site curve-fitting equation with Prism 6 (GraphPad Software) and K_i values were estimated from the Cheng−Prusoff equation.

4.4. Functional assays for 5-HT_6 receptor

Materials and methods. Test and reference compounds were dissolved in dimethyl sulfoxide (DMSO) at a concentration of 10 mM. Serial dilutions were prepared in 96-well microplate in assay buffer and 8 to 10 concentrations were tested. For the 5-HT6, adenylyl cyclase activity were monitored using cryopreserved 1321N1 cells with expression of the human serotonin 5-HT6 receptor (PerkinElmer, USA). Thawed cells were resuspended in stimulation buffer (HBSS, 5 mM HEPES, 0.5 IBMX, and 0.1% BSA at pH 7.4) at 3×10^5 cells/ml. The same volume (10 μl) of cell suspension was added to tested compounds. Samples were loaded onto a white opaque half area 96-well microplate. The antagonist response experiment was performed with 22 nM serotonin as the reference agonist for 5-HT6 receptor. The agonist and antagonist were added simultaneously. Cell stimulation was performed for 30 min at room temperature. After incubation, cAMP measurements were performed with homogeneous TR-FRET immunoassay using the LANCE Ultra cAMP kit (PerkinElmer, USA). 10 μl of EucAMP Tracer Working Solution and 10 μl of ULight-anti-cAMP Tracer Working Solution were added, mixed, and incubated for 1 h. The TR-FRET signal was read on an EnVision microplate reader (PerkinElmer, USA). IC_{50} and EC_{50} were determined by nonlinear regression analysis using GraphPad Prism 7.0 software.

4.5. Cholinesterases in vitro inhibitory activity (eeAChE, eqBuChE)

The reagents used to perform cholinesterases inhibitory activity assays were purchased from Sigma−Aldrich (Steinheim, Germany). The protocol based on spectrophotometric Ellman's method [68] was followed, with small modifications, using 96-well microplates. Aqueous stock solutions of the enzymes (eeAChE, eqBuChE) in the concentrations of 5U/mL were diluted before use, giving the final concentrations of 0.384 U/mL. Stock solutions of the tested compounds were prepared in DMSO. Prior to starting the reaction, the mixture of 25 μL of the target compound (or water or mixture of DMSO/water in appropriate ratio; i.e. blank samples) was incubated in 0.1 M phosphate buffer (200 μL, pH = 8.0) with DTNB (20 μL; 0.0025 M) and the enzyme (20 μL; eeAChE, eqBuChE). The incubation and final reactions were performed at room temperature (25 °C) for eeAChE or eqBuChE. After 5 min of pre-incubation, the final reactions were started by adding 20 μL of ATC (0.00375 M) or BTC (0.00375 M) solutions (depending on the enzyme used). Following the next 5 min, the changes in absorbance were measured at 412 nm, using a microplate reader (EnSpire Multimode; PerkinElmer, Waltham, MA, USA). All the target compounds were tested at the screening concentration of 10 μM. Based on equation 100-(S/B) × 100 (where S and B were the respective enzyme activities with and without the test sample, respectively) the percent of inhibition of each enzyme for each compound was calculated. Compounds with the enzyme inhibitory activity at 10 μM better than 50%, were further evaluated to obtain IC_{50} values. To determine IC_{50} value, seven different concentrations of each compound were tested giving enzyme inhibition between 5% and 95%. The experiments were performed in triplicate. The IC_{50} values were calculated using nonlinear regression (GraphPad Prism 5; GraphPad Software, San Diego, CA, USA) by plotting the residual enzyme activities against the applied inhibitor concentration. Tacrine, donepezil and rivastigmine were used as the reference compounds.

4.6. 100-Fold dilution assay

Following the modified protocol described by Kosak et al. [72], the recovery of eqBuChE activity was measured after 30 min, 60 min, and 120 min of the pre-incubation of the mixture containing 10-fold the IC_{50} of the target compound and 100-fold the final enzyme concentration (at room temperature 25 °C). After the pre-incubation time, 2.85 μL of mixture was diluted into each well's solution containing 242.15 μL of phosphate buffer (0.1 M; pH = 8) and 20 μL of DTNB (0.0025 M). Next, 20 μL of BTC (0.00375 M) was added, to start the final reaction. After 5 min, the absorbance was measured at 412 nm by a microplate reader (EnSpire Multimode; PerkinElmer, Waltham, MA, USA). Tacrine and donepezil (reversible enzyme inhibitors), as well as rivastigmine (pseudo-irreversible enzyme inhibitor), were used as the controls. The blank samples were prepared analogically to the tested ones, using preincubated enzyme with water mixture (or enzyme with appropriate ratio of water/DMSO) instead of the mixture of enzyme and the target compound. Two independent experiments were performed for the tested compounds, each one in quadruplicate.

4.7. In vitro $A\beta_{42}$aggregation inhibition - thioflavin-T (ThT) fluorometric assay [74]

The inhibition of $A\beta_{42}$ aggregation was measured fluorimetrically as described previously [85]. Briefly, HFIP-pretreated $A\beta_{42}$ (Merck Millipore, Darmstadt, Germany) at 1.5 μM, the test compound (10 μM final concentration) and Thioflavin-T (10 μM final concentration)

were incubated at room temperature in 96-well microplate covered with aluminum foil with continuous shaking for 24–48 h. The fluorescence intensity ($\lambda_{ex} = 440$ nm; $\lambda_{em} = 490$ nm) was measured every 3 min (Synergy™ H4 plate reader, BioTek Instruments, Inc. VT, USA). The assay was run in quadruplicates. For the IC_{50} determination, a serial dilution of compounds **17** and **35** were prepared (30 nM–30 μM, final concentrations). The percentage of inhibition was calculated as described above and the IC_{50} values were determined using GraphPad Prism 9.0 [GraphPad Software, San Diego, CA]). The IC_{50} values are reported as mean ± SEM of three independent experiments.

4.8. In cellulo $A\beta_{42}$ and tau aggregation inhibition - thioflavin-S (ThS) fluorometric assay

The assays were performed according to the previously described procedures [73,86,87]. **DP-128** was used as a reference compound [78]. Final data are the average of three independent experiments.

4.9. ADMET

General information. ADMET parameters of **17** and **35** were performed here according to described previously assays and protocols [79,88–91]. Statistical significances were analyzed by GraphPad Prism™ 8 software using One-way ANOVA and Bonferroni's Multiple Comparison Post Test. All references used during this study: caffeine (CFN), norfloxacin (Nfx), doxorubicin (DOX), ketoconazole (KE) and quinidine (QD) were obtained from Sigma-Aldrich (St. Louis, MO, USA).

4.9.1. Permeability PAMPA assay

Pre-coated PAMPA Plate System Gentest™ was obtained from Corning, (Tewksbury, MA, USA). The compounds and the references (CFN and Nfx) were tested at 200 μM. The used solutions were prepared in PBS buffer (pH = 7.4) and added to the donor wells (300 μL/well), whereas 200 μL/well of PBS was added to the acceptor wells. All compounds were analyzed in triplicate. The plate was incubated at room temperature for 5h. Then, the 50 μL was aspirated from each well and diluted next with 50 μl solution of an internal standard (IS). The compounds' concentrations in acceptor and donor wells were estimated by the UPLC-MS analyses performed by LC/MS Waters ACQUITY™ TQD system with the TQ Detector (Waters, Milford, USA). The permeability coefficients (Pe, cm/s) were calculated according described previously formulas [79].

4.9.2. Influence on CYP activity

The potential drug-drug interactions were predicted using CYP3A4 and CYP2D6 assays purchased from Promega (Madison, WI, USA). The compounds were tested in triplicate in following concentrations: 0.1, 1, 10 and 25 μM. The study was performed with use of the 1 μM concentration of respective reference CYP inhibitors: KE and QD.

4.9.3. Hepatotoxicity assays

Hepatotoxicity was estimated using hepatoma HepG2 (ATCC® HB-8065™) cell line. The CellTiter 96® AQueous Non-Radioactive Cell Proliferation Assay (MTS) used for estimation of cells viability was purchased from Promega (Madison, WI, USA). The compounds were tested in quadruplicate at four concentrations (1, 10, 50 and 100 μM) and incubated with cells for 48h. The antiproliferative drug DX in dose 1 μM and mitochondrial toxin CCCP (10 μM) were used as positive control.

4.9.4. Metabolic stability

The in silico prediction of most probable sites of metabolism was done by MetaSite 6.0.1 software (Molecular Discovery Ltd, Hertfordshire, UK).

The metabolic pathways determination *in vitro* was performed by 120 min compounds incubation with mouse liver microsomes (MLMs) purchased from Sigma-Aldrich, St. Louis, MO, USA. The reactions were conducted in 10 mM Tris–HCl buffer (pH 7.4) at 37 °C in the presence of NADPH Regeneration System (Promega, Madison, WI, USA). UPLC/MS analyses were done by Waters ACQUITY TQD system with the TQ Detector (Waters, Milford, USA).

Declaration of competing interest

The authors declare that they have no known competing financial interests or personal relationships that could have appeared to influence the work reported in this paper.

Acknowledgments

This work was supported by National Science Centre Poland (Grant No. 2016/23/D/NZ7/01328) and by Slovenian Research Agency – ARRS (research programme P1-0208 and project L1-8157). The presented mass spectrometry measurements were carried out in the Laboratory of Proteomics and Mass Spectrometry, Maj Institute of Pharmacology, Polish Academy of Sciences in Krakow, Poland.

Appendix A. Supplementary data

Supplementary data to this article can be found online at https://doi.org/10.1016/j.ejmech.2021.113783.

References

[1] L. Guzman-Martinez, C. Calfío, G.A. Farias, C. Vilches, R. Prieto, R.B. Maccioni, New frontiers in the prevention, diagnosis, and treatment of alzheimer's disease, J. Alzheimers. Dis. (2021), https://doi.org/10.3233/JAD-201059.
[2] 2020 Alzheimer's disease facts and figures, Alzheimer's Dementia 16 (2020) 391–460, https://doi.org/10.1002/alz.12068.
[3] R.A. Bekdash, The cholinergic system, the adrenergic system and the neuropathology of alzheimer's disease, Int. J. Mol. Sci. 22 (2021), https://doi.org/10.3390/ijms22031273.
[4] K.Y. Wong, J. Roy, M.L. Fung, B.C. Heng, C. Zhang, L.W. Lim, Relationships between mitochondrial dysfunction and neurotransmission failure in alzheimer's disease, Aging Dis 11 (2020) 1291–1316, https://doi.org/10.14336/AD.2019.1125.
[5] G.D. Stanciu, A. Luca, R.N. Rusu, V. Bild, S.I. Beschea Chiriac, C. Solcan, W. Bild, D.C. Ababei, Alzheimer's disease pharmacotherapy in relation to cholinergic system involvement, Biomolecules 10 (2019), https://doi.org/10.3390/biom10010040.
[6] D. Bertrand, T.L. Wallace, A review of the cholinergic system and therapeutic approaches to treat brain disorders, Curr. Top. Behav. Neurosci. 45 (2020) 1–28, https://doi.org/10.1007/7854_2020_141.
[7] E. Giacobini, Cholinesterase inhibitors: new roles and therapeutic alternatives, Pharmacol. Res. 50 (2004) 433–440, https://doi.org/10.1016/j.phrs.2003.11.017.
[8] A. Nordberg, C. Ballard, R. Bullock, T. Darreh-Shori, M. Somogyi, A review of butyrylcholinesterase as a therapeutic target in the treatment of Alzheimer's disease, Prim. Care Companion CNS Disord. 15 (2013), https://doi.org/10.4088/PCC.12r01412. PCC.12r01412.
[9] B.L. Klaassens, J.M.A. van Gerven, E.S. Klaassen, J. van der Grond, S.A.R.B. Rombouts, Cholinergic and serotonergic modulation of resting state functional brain connectivity in Alzheimer's disease, Neuroimage 199 (2019) 143–152, https://doi.org/10.1016/j.neuroimage.2019.05.044.
[10] C. Vakalopoulos, Alzheimer's disease: the alternative serotonergic hypothesis of cognitive decline, J. Alzheimers. Dis. 60 (2017) 859–866, https://doi.org/10.3233/JAD-170364.
[11] V.N. Bukke, M. Archana, R. Villani, A.D. Romano, A. Wawrzyniak, K. Balawender, S. Orkisz, S. Beggiato, G. Serviddio, T. Cassano, The dual role of glutamatergic neurotransmission in alzheimer's disease: from pathophysiology to pharmacotherapy, Int. J. Mol. Sci. 21 (2020), https://doi.org/10.3390/ijms21207452.
[12] G. Paroni, P. Bisceglia, D. Seripa, Understanding the amyloid hypothesis in

alzheimer's disease, J. Alzheimers. Dis. 68 (2019) 493–510, https://doi.org/10.3233/JAD-180802.
[13] G. Gallardo, D.M. Holtzman, Amyloid-β and tau at the crossroads of alzheimer's disease, Adv. Exp. Med. Biol. 1184 (2019) 187–203, https://doi.org/10.1007/978-981-32-9358-8_16.
[14] M.A. Busche, B.T. Hyman, Synergy between amyloid-β and tau in Alzheimer's disease, Nat. Neurosci. 23 (2020) 1183–1193, https://doi.org/10.1038/s41593-020-0687-6.
[15] S. Ayala, P. Genevaux, C. Hureau, P. Faller, (Bio)chemical strategies to modulate amyloid-β self-assembly, ACS Chem. Neurosci. 10 (2019) 3366–3374, https://doi.org/10.1021/acschemneuro.9b00239.
[16] L. Pinheiro, C. Faustino, Therapeutic strategies targeting amyloid-β in alzheimer's disease, Curr. Alzheimer Res. 16 (2019) 418–452, https://doi.org/10.2174/1567205016666190321163438.
[17] G. Caruso, S.F. Spampinato, V. Cardaci, F. Caraci, M.A. Sortino, S. Merlo, β-Amyloid and oxidative stress: perspectives in drug development, Curr. Pharmaceut. Des. 25 (2019) 4771–4781, https://doi.org/10.2174/1381612825666191209115431.
[18] D.A. Butterfield, D. Boyd-Kimball, Oxidative stress, amyloid-β peptide, and altered key molecular pathways in the pathogenesis and progression of alzheimer's disease, J. Alzheimers. Dis. 62 (2018) 1345–1367, https://doi.org/10.3233/JAD-170543.
[19] C. Cheignon, M. Tomas, D. Bonnefont-Rousselot, P. Faller, C. Hureau, F. Collin, Oxidative stress and the amyloid beta peptide in Alzheimer's disease, Redox Biol 14 (2018) 450–464, https://doi.org/10.1016/j.redox.2017.10.014.
[20] H. Watanabe, E. Bagarinao, T. Yokoi, H. Yamaguchi, S. Ishigaki, M. Mausuda, M. Katsuno, G. Sobue, Tau accumulation and network breakdown in alzheimer's disease, Adv. Exp. Med. Biol. 1184 (2019) 231–240, https://doi.org/10.1007/978-981-32-9358-8_19.
[21] S. Muralidar, S.V. Ambi, S. Sekaran, D. Thirumalai, B. Palaniappan, Role of tau protein in Alzheimer's disease: the prime pathological player, Int. J. Biol. Macromol. 163 (2020) 1599–1617, https://doi.org/10.1016/j.ijbiomac.2020.07.327.
[22] N.N. Naseri, H. Wang, J. Guo, M. Sharma, W. Luo, The complexity of tau in Alzheimer's disease, Neurosci. Lett. 705 (2019) 183–194, https://doi.org/10.1016/j.neulet.2019.04.022.
[23] M. Polydoro, C.M. Acker, K. Duff, P.E. Castillo, P. Davies, Age-dependent impairment of cognitive and synaptic function in the htau mouse model of tau pathology, J. Neurosci. 29 (2009) 10741–10749, https://doi.org/10.1523/JNEUROSCI.1065-09.2009.
[24] R. Morphy, C. Kay, Z. Rankovic, From magic bullets to designed multiple ligands, Drug Discov. Today 9 (2004) 641–651, https://doi.org/10.1016/S1359-6446(04)03163-0.
[25] R. Morphy, Z. Rankovic, Designed multiple ligands. An emerging drug discovery paradigm, J. Med. Chem. 48 (2005) 6523–6543, https://doi.org/10.1021/jm058225d.
[26] L. Blaikie, G. Kay, P. Kong Thoo Lin, Current and emerging therapeutic targets of alzheimer's disease for the design of multi-target directed ligands, Medchemcomm 10 (2019) 2052–2072, https://doi.org/10.1039/c9md00337a.
[27] R.R. Ramsay, M.R. Popovic-Nikolic, K. Nikolic, E. Uliassi, M.L. Bolognesi, A perspective on multi-target drug discovery and design for complex diseases, Clin. Transl. Med. 7 (2018) 3, https://doi.org/10.1186/s40169-017-0181-2.
[28] H.-H. Lin, L.-L. Zhang, R. Yan, J.-J. Lu, Y. Hu, Network analysis of drug-target interactions: a study on FDA-approved new molecular entities between 2000 to 2015, Sci. Rep. 7 (2017) 12230, https://doi.org/10.1038/s41598-017-12061-8.
[29] L. Blanco-Silvente, X. Castells, M. Saez, M.A. Barceló, J. Garre-Olmo, J. Vilalta-Franch, D. Capellà, Discontinuation, efficacy, and safety of cholinesterase inhibitors for alzheimer's disease: a meta-analysis and meta-regression of 43 randomized clinical trials enrolling 16 106 patients, Int. J. Neuropsychopharmacol. 20 (2017) 519–528, https://doi.org/10.1093/ijnp/pyx012.
[30] D. Panek, T. Wichur, J. Godyń, A. Pasieka, B. Malawska, Advances toward multifunctional cholinesterase and β-amyloid aggregation inhibitors, Future Med. Chem. 9 (2017), https://doi.org/10.4155/fmc-2017-0094.
[31] Q. Li, S. He, Y. Chen, F. Feng, W. Qu, H. Sun, Donepezil-based multi-functional cholinesterase inhibitors for treatment of Alzheimer's disease, Eur. J. Med. Chem. 158 (2018) 463–477, https://doi.org/10.1016/j.ejmech.2018.09.031.
[32] P. Mishra, A. Kumar, G. Panda, Anti-cholinesterase hybrids as multi-target-directed ligands against Alzheimer's disease (1998–2018), Bioorg. Med. Chem. 27 (2019) 895–930, https://doi.org/10.1016/j.bmc.2019.01.025.
[33] D.A. Rodríguez-Soacha, M. Scheiner, M. Decker, Multi-target-directed-ligands acting as enzyme inhibitors and receptor ligands, Eur. J. Med. Chem. 180 (2019) 690–706, https://doi.org/10.1016/j.ejmech.2019.07.040.
[34] G.A. Reid, N. Chilukuri, S. Darvesh, Butyrylcholinesterase and the cholinergic system, Neuroscience 234 (2013) 53–68, https://doi.org/10.1016/j.neuroscience.2012.12.054.
[35] J. Hartmann, C. Kiewert, E.G. Duysen, O. Lockridge, N.H. Greig, J. Klein, Excessive hippocampal acetylcholine levels in acetylcholinesterase-deficient mice are moderated by butyrylcholinesterase activity, J. Neurochem. 100 (2007) 1421–1429, https://doi.org/10.1111/j.1471-4159.2006.04347.x.
[36] B. Li, E.G. Duysen, M. Carlson, O. Lockridge, The butyrylcholinesterase knockout mouse as a model for human butyrylcholinesterase deficiency, J. Pharmacol. Exp. Therapeut. 324 (2008) 1146–1154, https://doi.org/10.1124/jpet.107.133330.
[37] U. Košak, B. Brus, D. Knez, R. Šink, S. Žakelj, J. Trontelj, A. Pišlar, J. Šlenc, M. Gobec, M. Živin, L. Tratnjek, M. Perše, K. Sałat, A. Podkowa, B. Filipek, F. Nachon, X. Brazzolotto, A. Więckowska, B. Malawska, J. Stojan, I.M. Raščan, J. Kos, N. Coquelle, J.-P. Colletier, S. Gobec, Development of an in-vivo active reversible butyrylcholinesterase inhibitor, Sci. Rep. 6 (2016) 39495, https://doi.org/10.1038/srep39495.
[38] S. Chakraborty, J.C. Lennon, S.A. Malkaram, Y. Zeng, D.W. Fisher, H. Dong, Serotonergic system, cognition, and BPSD in Alzheimer's disease, Neurosci. Lett. 704 (2019) 36–44, https://doi.org/10.1016/j.neulet.2019.03.050.
[39] J. Lalut, D. Karila, P. Dallemagne, C. Rochais, Modulating 5-HT4 and 5-HT6 receptors in Alzheimer's disease treatment, Future Med. Chem. 9 (2017) 781–795, https://doi.org/10.4155/fmc-2017-0031.
[40] S. Claeysen, J. Bockaert, P. Giannoni, Serotonin: a new hope in alzheimer's disease? ACS Chem. Neurosci. 6 (2015) 940–943, https://doi.org/10.1021/acschemneuro.5b00135.
[41] J. Lalut, H. Payan, A. Davis, C. Lecoutey, R. Legay, J. Sopkova-de Oliveira Santos, S. Claeysen, P. Dallemagne, C. Rochais, Rational design of novel benzisoxazole derivatives with acetylcholinesterase inhibitory and serotoninergic 5-HT(4) receptors activities for the treatment of Alzheimer's disease, Sci. Rep. 10 (2020) 3014, https://doi.org/10.1038/s41598-020-59805-7.
[42] C. Rochais, C. Lecoutey, K. Hamidouche, P. Giannoni, F. Gaven, E. Cem, S. Mignani, K. Baranger, T. Freret, J. Bockaert, S. Rivera, M. Boulouard, P. Dallemagne, S. Claeysen, Donecopride, a Swiss army knife with potential against Alzheimer's disease, Br. J. Pharmacol. 177 (2020) 1988–2005, https://doi.org/10.1111/bph.14964.
[43] C. Lanthier, H. Payan, I. Liparulo, B. Hatat, C. Lecoutey, M. Since, A. Davis, C. Bergamini, S. Claeysen, P. Dallemagne, M.-L. Bolognesi, C. Rochais, Novel multi target-directed ligands targeting 5-HT(4) receptors with in cellulo antioxidant properties as promising leads in Alzheimer's disease, Eur. J. Med. Chem. 182 (2019) 111596, https://doi.org/10.1016/j.ejmech.2019.111596.
[44] B. Hatat, S. Yahiaoui, C. Lecoutey, A. Davis, T. Freret, M. Boulouard, S. Claeysen, C. Rochais, P. Dallemagne, A novel in vivo anti-amnesic agent, specially designed to express both acetylcholinesterase (AChE) inhibitory, serotonergic subtype 4 receptor (5-HT(4)R) agonist and serotonergic subtype 6 receptor (5-HT(6)R) inverse agonist activities, with a potential I, Front. Aging Neurosci. 11 (2019) 148, https://doi.org/10.3389/fnagi.2019.00148.
[45] S. Yahiaoui, K. Hamidouche, C. Ballandonne, A. Davis, J.S. de Oliveira Santos, T. Freret, M. Boulouard, C. Rochais, P. Dallemagne, Design, synthesis, and pharmacological evaluation of multitarget-directed ligands with both serotonergic subtype 4 receptor (5-HT 4 R) partial agonist and 5-HT6R antagonist activities, as potential treatment of Alzheimer's disease, Eur. J. Med. Chem. 121 (2016) 283–293, https://doi.org/10.1016/j.ejmech.2016.05.048.
[46] E.S. Mitchell, J.F. Neumaier, 5-HT6 receptors: a novel target for cognitive enhancement, Pharmacol. Ther. 108 (2005) 320–333, https://doi.org/10.1016/j.pharmthera.2005.05.001.
[47] K.C.F. Fone, An update on the role of the 5-hydroxytryptamine6 receptor in cognitive function, Neuropharmacology 55 (2008) 1015–1022, https://doi.org/10.1016/j.neuropharm.2008.06.061.
[48] B. Marcos, F.J. Gil-Bea, W.D. Hirst, M. García-Alloza, M.J. Ramírez, Lack of localization of 5-HT6 receptors on cholinergic neurons: implication of multiple neurotransmitter systems in 5-HT6 receptor-mediated acetylcholine release, Eur. J. Neurosci. 24 (2006) 1299–1306, https://doi.org/10.1111/j.1460-9568.2006.05003.x.
[49] C. Riemer, E. Borroni, B. Levet-Trafit, J.R. Martin, S. Poli, R.H.P. Porter, M. Bös, Influence of the 5-HT6 receptor on acetylcholine release in the cortex: pharmacological characterization of 4-(2-bromo-6-pyrrolidin-1-ylpyridine-4-sulfonyl)phenylamine, a potent and selective 5-HT6 receptor antagonist, J. Med. Chem. 46 (2003) 1273–1276, https://doi.org/10.1021/jm021085c.
[50] A. Bali, S. Singh, Serotonergic 5-HT6 receptor antagonists: heterocyclic chemistry and potential therapeutic significance, Curr. Top. Med. Chem. 15 (2015) 1643–1662, https://doi.org/10.2174/1568026615666150427110420.
[51] L.A. Dawson, H.Q. Nguyen, P. Li, The 5-HT6 receptor antagonist SB-271046 selectively enhances excitatory neurotransmission in the rat frontal cortex and hippocampus, Neuropsychopharmacology 25 (2001) 662–668, https://doi.org/10.1016/S0893-133X(01)00265-2.
[52] L.E. Schechter, Q. Lin, D.L. Smith, G. Zhang, Q. Shan, B. Platt, M.R. Brandt, L.A. Dawson, D. Cole, R. Bernotas, A. Robichaud, S. Rosenzweig-Lipson, C.E. Beyer, Neuropharmacological profile of novel and selective 5-HT6 receptor agonists: WAY-181187 and WAY-208466, Neuropsychopharmacology 33 (2008) 1323–1335, https://doi.org/10.1038/sj.npp.1301503.
[53] H.-M. Yun, H. Rhim, The serotonin-6 receptor as a novel therapeutic target, Exp. Neurobiol. 20 (2011) 159, https://doi.org/10.5607/en.2011.20.4.159.
[54] P.J. West, V.R. Marcy, M.J. Marino, H. Schaffhauser, Activation of the 5-HT6 receptor attenuates long-term potentiation and facilitates GABAergic neurotransmission in rat hippocampus, Neuroscience 164 (2009) 692–701, https://doi.org/10.1016/j.neuroscience.2009.07.061.
[55] M.L. Woolley, C.A. Marsden, K.C.F. Fone, 5-HT6 receptors, Curr. Drug Targets - CNS Neurol. Disord. 3 (2004) 59–79, https://doi.org/10.2174/1568007043482561.
[56] A. Wesołowska, Potential role of the 5-HT6 receptor in depression and anxiety: an overview of preclinical data, Pharmacol. Rep. 62 (2010) 564–577, https://doi.org/10.1016/s1734-1140(10)70315-7.
[57] H. Ferrero, M. Solas, P.T. Francis, M.J. Ramirez, Serotonin 5-HT6 receptor antagonists in Alzheimer's disease: therapeutic rationale and current development status, CNS Drugs 31 (2017) 19–32, https://doi.org/10.1007/s40263-016-0399-3.

[58] A.G. Foley, W.D. Hirst, H.C. Gallagher, C. Barry, J.J. Hagan, N. Upton, F.S. Walsh, A.J. Hunter, C.M. Regan, The selective 5-HT6 receptor antagonists SB-271046 and SB-399885 potentiate NCAM PSA immunolabeling of dentate granule cells, but not neurogenesis, in the hippocampal formation of mature Wistar rats, Neuropharmacology 54 (2008) 1166–1174, https://doi.org/10.1016/j.neuropharm.2008.03.012.
[59] C. Routledge, S.M. Bromidge, S.F. Moss, G.W. Price, W. Hirst, H. Newman, G. Riley, T. Gager, T. Stean, N. Upton, S.E. Clarke, A.M. Brown, D.N. Middlemiss, Characterization of SB-271046: a potent, selective and orally active 5-HT(6) receptor antagonist, Br. J. Pharmacol. 130 (2000) 1606–1612, https://doi.org/10.1038/sj.bjp.0703457.
[60] A. Calhoun, J. Ko, G.T. Grossberg, Emerging chemical therapies targeting 5-hydroxytryptamine in the treatment of Alzheimer's disease, Expet Opin. Emerg. Drugs 22 (2017) 101–105, https://doi.org/10.1080/14728214.2017.1293651.
[61] D. Wilkinson, K. Windfeld, E. Colding-Jørgensen, Safety and efficacy of idalopirdine, a 5-HT6 receptor antagonist, in patients with moderate Alzheimer's disease (LADDER): a randomised, double-blind, placebo-controlled phase 2 trial, Lancet Neurol. 13 (2014) 1092–1099, https://doi.org/10.1016/S1474-4422(14)70198-X.
[62] A. Milelli, A. De Simone, N. Ticchi, H.H. Chen, N. Betari, V. Andrisano, V. Tumiatti, Tacrine-based multifunctional agents in alzheimer's disease: an old story in continuous development, Curr. Med. Chem. 24 (2017) 3522–3546, https://doi.org/10.2174/0929867324666170309123920.
[63] H. Lin, Q. Li, K. Gu, J. Zhu, X. Jiang, Y. Chen, H. Sun, Therapeutic agents in alzheimer's disease through a multi-targetdirected ligands strategy: recent progress based on tacrine core, Curr. Top. Med. Chem. 17 (2017) 3000–3016, https://doi.org/10.2174/1568026617666170717114944.
[64] J. Korabecny, K. Spilovska, E. Mezeiova, O. Benek, R. Juza, D. Kaping, O. Soukup, A systematic review on donepezil-based derivatives as potential cholinesterase inhibitors for alzheimer's disease, Curr. Med. Chem. 26 (2019) 5625–5648, https://doi.org/10.2174/0929867325666180517094023.
[65] J. Wu, M. Pistolozzi, S. Liu, W. Tan, Design, synthesis and biological evaluation of novel carbamates as potential inhibitors of acetylcholinesterase and butyrylcholinesterase, Bioorg. Med. Chem. 28 (2020) 115324, https://doi.org/10.1016/j.bmc.2020.115324.
[66] A. Więckowska, M. Kołaczkowski, A. Bucki, J. Godyń, M. Marcinkowska, K. Więckowski, P. Zaręba, A. Siwek, G. Kazek, M. Głuch-Lutwin, P. Mierzejewski, P. Bienkowski, H. Sienkiewicz-Jarosz, D. Knez, T. Wichur, S. Gobec, B. Malawska, Novel multi-target-directed ligands for Alzheimer's disease: combining cholinesterase inhibitors and 5-HT6 receptor antagonists. Design, synthesis and biological evaluation, Eur. J. Med. Chem. 124 (2016) 63–81, https://doi.org/10.1016/j.ejmech.2016.08.016.
[67] A. Więckowska, T. Wichur, J. Godyń, A. Bucki, M. Marcinkowska, A. Siwek, K. Więckowski, P. Zaręba, D. Knez, M. Głuch-Lutwin, G. Kazek, G. Latacz, K. Mika, M. Kołaczkowski, J. Korabecny, O. Soukup, M. Benkova, K. Kieć-Kononowicz, S. Gobec, B. Malawska, Novel multitarget-directed ligands aiming at symptoms and causes of alzheimer's disease, ACS Chem. Neurosci. 9 (2018), https://doi.org/10.1021/acschemneuro.8b00024.
[68] G.L. Ellman, K.D. Courtney, V. Andres, R.M. Featherstone, A new and rapid colorimetric determination of acetylcholinesterase activity, Biochem. Pharmacol. 7 (1961) 88–95, https://doi.org/10.1016/0006-2952(61)90145-9.
[69] M. Kołaczkowski, M. Marcinkowska, A. Bucki, M. Pawłowski, K. Mitka, J. Jaśkowska, P. Kowalski, G. Kazek, A. Siwek, A. Wasik, A. Wesołowska, P. Mierzejewski, P. Bienkowski, Novel arylsulfonamide derivatives with 5-HT6/5-HT7 receptor antagonism targeting behavioral and psychological symptoms of dementia, J. Med. Chem. 57 (2014) 4543–4557, https://doi.org/10.1021/jm401895u.
[70] C. Wang, Y. Jiang, J. Ma, H. Wu, D. Wacker, V. Katritch, G.W. Han, W. Liu, X.P. Huang, E. Vardy, J.D. McCorvy, X. Gao, X.E. Zhou, K. Melcher, C. Zhang, F. Bai, H. Yang, L. Yang, H. Jiang, B.L. Roth, V. Cherezov, R.C. Stevens, H.E. Xu, Structural basis for molecular recognition at serotonin receptors, Science (Washington, D.C.) 340 (2013) 610–614, https://doi.org/10.1126/science.1232807.
[71] A. Bucki, M. Marcinkowska, J. Śniecikowska, K. Więckowski, M. Pawłowski, M. Głuch-Lutwin, A. Gryboś, A. Siwek, K. Pytka, M. Jastrzębska-Więsek, A. Partyka, A. Wesołowska, P. Mierzejewski, M. Kołaczkowski, Novel 3-(1,2,3,6-Tetrahydropyridin-4-yl)-1H-indole-Based multifunctional ligands with antipsychotic-like, mood-modulating, and procognitive activity, J. Med. Chem. 60 (2017) 7483–7501, https://doi.org/10.1021/acs.jmedchem.7b00839.
[72] U. Košak, N. Strašek, D. Knez, M. Jukič, S. Žakelj, A. Zahirović, A. Pišlar, X. Brazzolotto, F. Nachon, J. Kos, S. Gobec, N-alkylpiperidine carbamates as potential anti-Alzheimer's agents, Eur. J. Med. Chem. 197 (2020) 112282, https://doi.org/10.1016/j.ejmech.2020.112282.
[73] N. Szałaj, J. Godyń, J. Jończyk, A. Pasieka, D. Panek, T. Wichur, K. Więckowski, P. Zaręba, M. Bajda, A. Pislar, B. Malawska, R. Sabate, A. Więckowska, Multidirectional in vitro and in cellulo studies as a tool for identification of multi-target-directed ligands aiming at symptoms and causes of Alzheimer's disease, J. Enzym. Inhib. Med. Chem. 35 (2020) 1944–1952, https://doi.org/10.1080/14756366.2020.1835882.
[74] H. LeVine, Thioflavine T interaction with synthetic Alzheimer's disease beta-amyloid peptides: detection of amyloid aggregation in solution, Protein Sci. 2 (1993) 404–410, https://doi.org/10.1002/pro.5560020312.
[75] A. Espargaró, A. Medina, O. Di Pietro, D. Muñoz-Torrero, R. Sabate, Ultra rapid in vivo screening for anti-Alzheimer anti-amyloid drugs, Sci. Rep. 6 (2016) 1–8, https://doi.org/10.1038/srep23349.
[76] A. Espargaró, T. Ginex, M. del M. Vadell, M.A. Busquets, J. Estelrich, D. Muñoz-Torrero, F.J. Luque, R. Sabate, Combined in vitro cell-based/in silico screening of naturally occurring flavonoids and phenolic compounds as potential anti-alzheimer drugs, J. Nat. Prod. 80 (2017) 278–289, https://doi.org/10.1021/acs.jnatprod.6b00643.
[77] A. Pasieka, D. Panek, J. Jończyk, J. Godyń, N. Szałaj, G. Latacz, J. Tabor, E. Mezeiova, F. Chantegreil, J. Dias, D. Knez, J. Lu, R. Pi, J. Korabecny, X. Brazzolotto, S. Gobec, G. Höfner, K. Wanner, A. Więckowska, B. Malawska, Discovery of multifunctional anti-Alzheimer's agents with a unique mechanism of action including inhibition of the enzyme butyrylcholinesterase and γ-aminobutyric acid transporters, Eur. J. Med. Chem. 218 (2021) 113397, https://doi.org/10.1016/j.ejmech.2021.113397.
[78] O. Di Pietro, F.J. Pérez-Areales, J. Juárez-Jiménez, A. Espargaró, M.V. Clos, B. Pérez, R. Lavilla, R. Sabaté, F.J. Luque, D. Muñoz-Torrero, Tetrahydrobenzo[h][1,6]naphthyridine-6-chlorotacrine hybrids as a new family of anti-Alzheimer agents targeting β-amyloid, tau, and cholinesterase pathologies, Eur. J. Med. Chem. 84 (2014) 107–117, https://doi.org/10.1016/j.ejmech.2014.07.021.
[79] X. Chen, A. Murawski, K. Patel, C.L. Crespi, P. V Balimane, A novel design of artificial membrane for improving the PAMPA model, Pharm. Res. (N. Y.) 25 (2008) 1511–1520, https://doi.org/10.1007/s11095-007-9517-8.
[80] B.P. Smart, R.C. Oslund, L.A. Walsh, M.H. Gelb, The first potent inhibitor of mammalian group X secreted phospholipase A2: elucidation of sites for enhanced binding, J. Med. Chem. 49 (2006) 2858–2860, https://doi.org/10.1021/jm060136t.
[81] R. Clark, S.-H. Zhao, 1-Sulfonyl-4-aminoalkoxyindole derivatives and uses thereof, U.S. Patent 2003/0229069 A1 (2003).
[82] P. Zhou, Y. Yan, R. Bernotas, B.L. Harrison, D. Huryn, A.J. Robichaud, G.M. Zhang, D.L. Smith, L.E. Schechter, 4-(2-Aminoethoxy)-N-(phenylsulfonyl) indoles as novel 5-HT6 receptor ligands, Bioorg. Med. Chem. Lett 15 (2005) 1393–1396, https://doi.org/10.1016/j.bmcl.2005.01.005.
[83] M. Kołaczkowski, A. Bucki, M. Feder, M. Pawłowski, Ligand-optimized homology models of D1 and D2 dopamine receptors: application for virtual screening, J. Chem. Inf. Model. 53 (2013) 638–648, https://doi.org/10.1021/ci300413h.
[84] C. Wang, Y. Jiang, J. Ma, H. Wu, D. Wacker, V. Katritch, G.W. Han, W. Liu, X.-P. Huang, E. Vardy, J.D. McCorvy, X. Gao, X.E. Zhou, K. Melcher, C. Zhang, F. Bai, H. Yang, L. Yang, H. Jiang, B.L. Roth, V. Cherezov, R.C. Stevens, H.E. Xu, Structural basis for molecular recognition at serotonin receptors, Science 340 (2013) 610–614, https://doi.org/10.1126/science.1232807.
[85] M. Hebda, M. Bajda, A. Więckowska, N. Szałaj, A. Pasieka, D. Panek, J. Godyń, T. Wichur, D. Knez, S. Gobec, B. Malawska, Synthesis, molecular modelling and biological evaluation of novel heterodimeric, multiple ligands targeting cholinesterases and amyloid beta, Molecules 21 (2016) 410, https://doi.org/10.3390/molecules21040410.
[86] D. Muñoz-Torrero, R. Sabate, S. Pouplana, A. Espargaro, C. Galdeano, E. Viayna, I. Sola, S. Ventura, Thioflavin-S staining of bacterial inclusion bodies for the fast, simple, and inexpensive screening of amyloid aggregation inhibitors, Curr. Med. Chem. 21 (2014) 1152–1159, https://doi.org/10.2174/0929867313206660256.
[87] T. Wichur, A. Więckowska, K. Więckowski, J. Godyń, J. Jończyk, Á.R. Valdivieso, D. Panek, A. Pasieka, R. Sabaté, D. Knez, S. Gobec, B. Malawska, 1-Benzylpyrrolidine-3-amine-based BuChE inhibitors with anti-aggregating, antioxidant and metal-chelating properties as multifunctional agents against Alzheimer's disease, Eur. J. Med. Chem. 187 (2020), https://doi.org/10.1016/j.ejmech.2019.111916.
[88] G. Latacz, A. Lubelska, M. Jastrzębska-Więsek, A. Partyka, M.A. Marć, G. Satała, D. Wilczyńska, M. Kotańska, M. Więcek, K. Kamińska, A. Wesołowska, K. Kieć-Kononowicz, J. Handzlik, The 1,3,5-triazine derivatives as innovative chemical family of 5-HT6 serotonin receptor agents with therapeutic perspectives for cognitive impairment, Int. J. Mol. Sci. 20 (2019), https://doi.org/10.3390/ijms20143420.
[89] G. Latacz, A.S. Hogendorf, A. Hogendorf, A. Lubelska, J.M. Wierońska, M. Woźniak, P. Cieślik, K. Kieć-Kononowicz, J. Handzlik, A.J. Bojarski, Search for a 5-CT alternative. In vitro and in vivo evaluation of novel pharmacological tools: 3-(1-alkyl-1H-imidazole-5-yl)-1H-indole-5-carboxamides, low-basicity 5-HT(7) receptor agonists, Medchemcomm 9 (2018) 1882–1890, https://doi.org/10.1039/c8md00313k.
[90] A. Lubelska, G. Latacz, M. Jastrzębska-Więsek, M. Kotańska, R. Kurczab, A. Partyka, M.A. Marć, D. Wilczyńska, A. Doroz-Płonka, D. Łażewska, A. Wesołowska, K. Kieć-Kononowicz, J. Handzlik, Are the hydantoin-1,3,5-triazine 5-HT(6)R ligands a hope to a find new procognitive and anti-obesity drug? Considerations based on primary in vivo assays and ADME-tox profile in vitro, Molecules 24 (2019), https://doi.org/10.3390/molecules24244472.
[91] A. Więckowska, N. Szałaj, I. Góral, A. Bucki, G. Latacz, K. Kiec-Kononowicz, Ò.M. Bautista-Aguilera, A. Romero, E. Ramos, J. Egea, V. Farré Alíns, Á. González-Rodríguez, F. López-Muñoz, M. Chioua, J. Marco-Contelles, In vitro and in silico ADME-tox profiling and safety significance of multifunctional monoamine oxidase inhibitors targeting neurodegenerative diseases, ACS Chem. Neurosci. 11 (2020) 3793–3801, https://doi.org/10.1021/acschemneuro.0c00489.